Space Radiation

Risk of Radiation Carcinogenesis

Risk of Acute Radiation Syndromes Due to Solar Particle Events

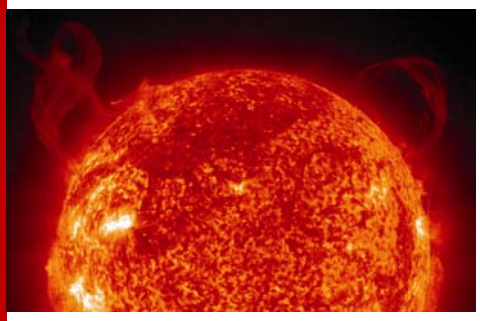

Risk of Acute or Late Central Nervous System Effects from Radiation Exposure

Risk of Degenerative Tissue or Other Health Effects from Radiation Exposure

Chapter 4:
Risk of Radiation Carcinogenesis

Francis A. Cucinotta
NASA Johnson Space Center

Marco Durante
GSI Germany

Occupational radiation exposure from the space environment may increase cancer morbidity or mortality risk in astronauts. This risk may be influenced by other space flight factors including microgravity and environmental contaminants. A Mars mission will not be feasible unless improved shielding is developed or transit time is decreased. – *Human Research Program Requirements Document*, HRP-47052, Rev. C, dated Jan 2009.

Pictured is the Crab Nebula, a 6-light-year-wide expanding remnant of the supernova explosion of a star; the colors indicate the different expelled elements. Astronauts in space are exposed to protons and high-energy and charge ions that are released by events such as supernovae, along with secondary radiation, including neutrons and recoil nuclei that are produced by nuclear reactions in spacecraft and tissue. Ground studies and system biology models of cancer risk reduce uncertainties in risk projection models and pave the way for biological countermeasure development to protect astronauts on future Exploration missions.

Executive Summary

Astronauts who are on missions to the ISS, the moon, or Mars are exposed to ionizing radiation with effective doses in the range from 50 to 2,000 mSv (milli-Sievert) as projected for possible mission scenarios (Cucinotta and Durante, 2006; Cucinotta et al., 2008). The evidence of cancer risk from ionizing radiation is extensive for radiation doses that are above about 50 mSv. Human epidemiology studies that provide evidence for cancer risks for low-linear energy transfer (LET) radiation such as X rays or gamma rays at doses from 50 to 2,000 mSv include: the survivors of the atomic-bomb explosions in Hiroshima and Nagasaki, nuclear reactor workers (Cardis et al., 1995; 2007) in the United States, Canada, Europe, and Russia, and patients who were treated therapeutically with radiation. Ongoing studies are providing new evidence of radiation cancer risks in populations that were accidentally exposed to radiation (i.e., from the Chernobyl accident and from Russian nuclear weapons production sites), and continue to analyze results from the Japanese atomic-bomb survivors from Hiroshima and Nagasaki. These studies provide strong evidence for cancer morbidity and mortality risks at more than 12 tissue sites, with the largest cancer risks for adults found for leukemia and tumors of the lung, breast, stomach, colon, bladder, and liver. There is also strong evidence for inter-gender variations due to differences in the natural incidence of cancer as well as additional cancer risks for the breast and the ovaries and a higher risk from radiation for lung cancer in females (National Council on Radiation Protection and Measurements (NCRP), 2000). Human studies also provide evidence for a declining risk with increasing age at exposure, although the magnitude of this reduction above age 30 years is uncertain (NCRP, 2000; Biological Effects of Ionizing Radiation (BEIR), 2006). Genetic and environmental factors that contribute to radiation carcinogenesis are also being explored to support the identification of individuals with higher or reduced risk.

In space, astronauts are exposed to protons and high-Z high-energy (HZE) ions together with secondary radiation, including neutrons and recoil nuclei, which are produced by nuclear reactions in spacecraft or tissue. Whole body doses of 1 to 2 mSv/day accumulate in interplanetary space, and approximately half of this value accumulates on planetary surfaces (Cucinotta et al., 2006; NCRP, 2006). Radiation shielding is an effective countermeasure for solar particle events (SPEs), which are chiefly made up of protons with energies that are largely below a few hundred MeV. The intermediate dose-rates (<500 mSv/hour) and scarcity of data on the biological effectiveness of protons as compared to low-LET radiation make optimization of SPE shielding uncertain at this time, however. The energy spectrum of galactic cosmic rays (GCRs) peaks near 1,000 MeV/nucleon; consequently, these particles are so penetrating that shielding can only partially reduce the doses that are absorbed by the crew (Cucinotta et al., 2006). Thick shielding poses obvious mass problems to spacecraft launch systems, and would only reduce the GCR effective dose by no more than 25% using aluminum, or about 35% using more efficient polyethylene. Therefore, with the exception of solar proton events, which are effectively absorbed by shielding, current shielding approaches cannot be considered a solution for the space radiation problem (Cucinotta et al., 2006; Wilson et al., 1995). In traveling to Mars, every cell nucleus within an astronaut would be traversed by a proton or secondary electron every few days, and by an HZE ion every few months (Cucinotta et al., 1998b). The large ionization power of HZE ions makes them the major contributor to the risk, in spite of their lower cell nucleus hit frequency compared to protons.

Epidemiological data, which are largely derived from the atomic-bomb survivors in Japan (Preston et al., 2003), provide a basis for risk estimation for low-LET radiation. However, because no human data exist for protons and HZE ions, space risk estimates must rely entirely on experimental model systems and biophysical considerations. Projections to predict cancer risks in astronauts are currently made using the double detriment life-table for an average population such as is found in the U.S., which is made up of age- and gender-dependent rates of death from cancer and all causes of death combined with a model of radiation cancer mortality rate (NCRP, 2000). The model that is used for the radiation cancer mortality rate is based on epidemiological studies of atomic-bomb survivors, which are assumed to be scalable to other populations, dose-rates, and radiation types.

The two scaling parameters with large uncertainties are the radiation quality factor, which estimates the increased effectiveness of HZE nuclei as compared to gamma rays for the same dose, and the dose- and dose-rate effectiveness factor (DDREF). The DDREF estimates the reduction of a risk at low doses (<200 mGy) or dose-rates (<0.05 Gy/hour) compared to an acute exposure. Maximum acceptable levels of risk for astronauts are typically set at a 3% fatal risk (Cucinotta and Durante, 2006; NCRP, 1997b; 2000), but the large uncertainties in projections and the likelihood of other fatal or morbidity risks for degenerative diseases precludes a go/no-go decision at this time for Mars exploration. The scaling of mortality rates for space radiation risks to astronauts to the atomic-bomb survivors introduces many uncertainties into risk estimates (Cucinotta et al., 2001; Cucinotta and Durante, 2006), and there are also important questions with regard to the correctness of any scaling approach because of qualitative differences in the biological effects of HZE ions and gamma rays.

Acceptable levels of risk must be guided by societal or ethical norms. Debate continues on what level is acceptable for space radiation cancer risks for the exploration of the moon or Mars. Although a historical perspective is summarized herein, we note that the strong possibility of non-cancer mortality and morbidity risks must also be considered for a Mars mission. Improvements in safety in other areas of space flight should place pressure on radiation protection to improve and lower the risks to astronauts from space radiation.

Ground-based experimentation (Durante and Cucinotta, 2008) is key to solving the problem of space radiation cancer risk estimation because flight experiments are difficult, expensive, and poorly reproducible; the dose-rate is too low to get useful data in reasonable time; and, in the past, experiments have yielded no major findings (Kiefer and Pross, 1999; Schimmerling et al., 2003; Durante and Kronenberg, 2005). As part of its Space Radiation Program, NASA has invested in the NASA Space Radiation Laboratory (NSRL) at Brookhaven National Laboratory (Upton, N.Y.) to simulate the high-energy protons and heavy ions that are found in space. NSRL, which opened for research in October 2003, has produced experimental data in the past few years that are of great relevance for reducing uncertainty on risk assessment.

Although studies with animals are an important component of space radiation research, they are time-consuming and expensive in light of the large number of radiation types, doses, and dose-rates that are of concern to NASA. Systems biology models of cancer risk that can be used to extrapolate radiation quality over the broad range of nuclear types and energies and fluence rates in space suggest that effective mitigation measures are a promising new approach to these problems. Mechanistic research performed at NSRL with two-dimensional (2D) human cell culture and three-dimensional (3D) human coculture models (Barcellos-Hoff et al., 2005) as well as animal studies in murine models is being pursued to establish level of risk, reduce uncertainties in risk projection models, guide the extrapolation from experiment to astronauts, and pave the way for biological countermeasure development (Cucinotta and Durante, 2006).

Introduction

As noted by Durante and Cucinotta (2008), cancer risk that is caused by exposure to space radiation is now generally considered the main hindrance to interplanetary travel for the following reasons: large uncertainties are associated with the projected cancer risk estimates; no simple and effective countermeasures are available, and significant uncertainties prevent scientists from determining the effectiveness of countermeasures. Optimizing operational parameters such as the length of space missions, crew selection for age and gender, or applying mitigation measures such as radiation shielding or use of biological countermeasures can be used to reduce risk, but these procedures are clouded by uncertainties.

Space radiation is comprised of high-energy protons and high-charge (Z) and -energy (E) nuclei (HZE) whose ionization patterns in molecules, cells, and tissues, and the resulting initial biological insults, are distinct from typical terrestrial radiation, which consists largely of X rays and gamma rays that are characterized as low-LET radiation. GCRs, which originate outside of our galaxy (probably from supernovas), are comprised mostly of highly energetic protons with a small component of HZE. Prominent HZE nuclei include: helium (He), carbon (C), oxygen (O), neon (Ne), magnesium (Mg), silicon (Si), and iron (Fe). GCR energy spectra peaks, which have median energies of about 1,000 MeV/amu, and nuclei with energies as high as 10,000 MeV/amu, make important contributions to the dose-equivalent.

Ionizing radiation is a well-known carcinogen on Earth (BEIR, 2006). The risks of cancer from X rays and gamma rays have been established at doses above 50 mSv (5 rem), although there are important uncertainties and ongoing scientific debate concerning cancer risk at lower doses and at low dose-rates (<50 mSv/hour). The relationship between the early biological effects of HZE nuclei and the probability of cancer in humans is poorly understood, and it is this missing knowledge that leads to significant uncertainties in projecting cancer risks during space exploration (Cucinotta and Durante, 2006; Durante and Cucinotta, 2008).

Uncertainties in cancer projections

For space radiation risk assessments, the major uncertainties in cancer prediction are

- Radiation quality effects on biological damage related to the qualitative and quantitative differences between space radiation compared to X rays
- Dependence of risk on dose-rates in space related to the biology of deoxyribonucleic acid (DNA) repair, cell regulation, and tissue or organism responses
- Predicting SPEs, including temporal, energy spectra, and size predictions
- Extrapolation from experimental data to humans and between human populations
- Individual radiation-sensitivity factors, including genetic, epigenetic, dietary, or “healthy worker” effects

The minor uncertainties in cancer risk prediction are

- Data on GCR environments
- Physics of shielding assessments related to transmission properties of radiation through materials and tissue
- Microgravity effects on biological responses to radiation
- Errors in human data (statistical, dosimetry, or recording inaccuracies)

Quantitative methods have been developed to propagate uncertainties for the several factors that contribute to cancer risk estimates (NCRP, 1997a; Cucinotta et al., 2001; 2006). A description of uncertainty analysis using Monte Carlo techniques is provided below. Current estimates of levels of uncertainty, which are represented as fold changes of the upper 95% confidence interval (C.I.) over the median risk projection, are illustrated in figure 4-1, and a comparison of the risks for adults for both terrestrial and space exposures is shown in figure 4-2. The contribution of microgravity effects on space radiation risk has not yet been estimated but it is expected to be small (Kiefer and Pross, 1999). Changes in oxygen levels or in immune dysfunction (Smyth et al., 2006) are of concern during space flight. Their effects on radiation cancer risks are largely unknown.

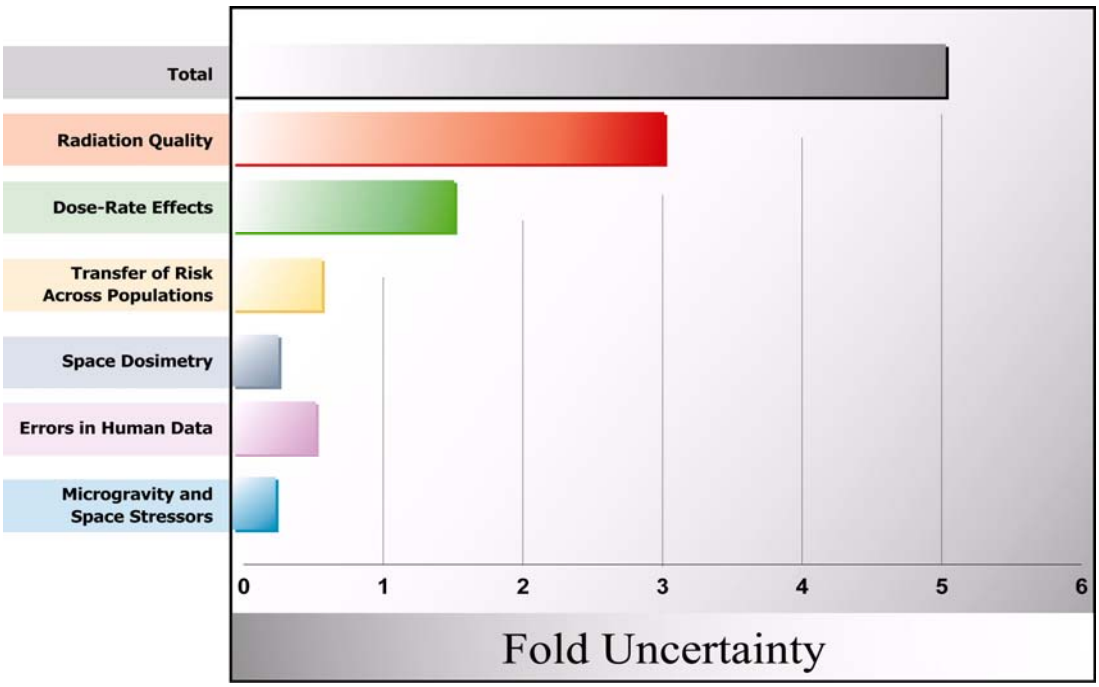

Figure 4-1. ***Estimates of fold uncertainties from several factors that contribute to cancer risk estimates from space radiation exposures. The uncertainties are larger for astronauts who are in space as compared to typical exposures on Earth, as illustrated.***

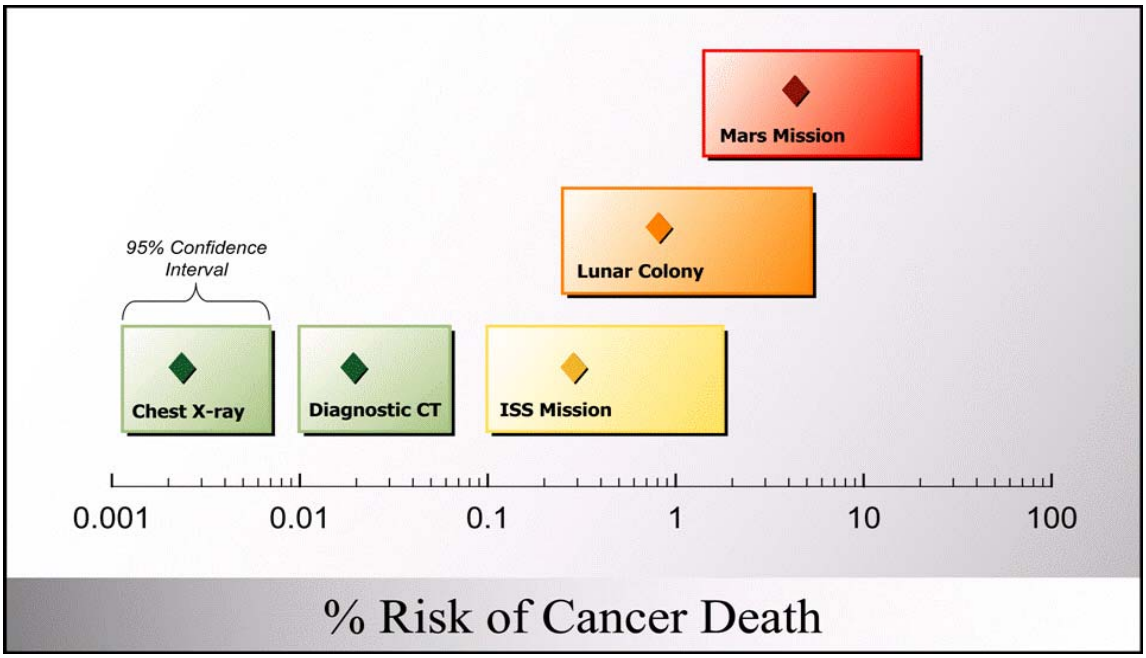

Figure 4-2. ***Uncertainties in risk projection for terrestrial and space exposures. The uncertainties are larger for astronauts who are in space as compared to typical exposures on Earth, as illustrated here. This figure shows the current estimates of cancer risks (diamonds) and 95% confidence bands for adults of age 40 years, which is the typical age of astronauts on space missions, for several terrestrial exposures and missions on the ISS as well as projections for a lunar colony and a Mars mission.***

Radiation affects cells and tissues either through direct damage to the cellular components or through the production of highly reactive free radicals from water (Goodhead, 1994). Both of these mechanisms can generate sufficient damage to cause cellular death, DNA mutation, or abnormal cellular function. The extent of damage is generally believed to be dependent on the dose and type of particle with a linear dose-response curve (Goodhead, 1994). This is true for high and moderate radiation exposure, but it is extremely difficult to measure for lower doses where it is not easy to discern the effects of radiation exposure from those that are triggered by the normal oxidative stress with which cells and tissues deal constantly. The HZE nuclei are unique components of space radiation that produce densely ionizing tracks as they pass through matter; when they traverse a biological system, they leave streaks or tracks of damage at the biomolecular level that fundamentally differ from the damage that is left by low-LET radiation sources such as gamma rays and X rays. In the nucleus of a cell, where the genetic material is stored, the traversal of a heavy ion can produce tracks of clustered DNA damage (Cucinotta and Durante, 2006), as illustrated in figure 4-3.

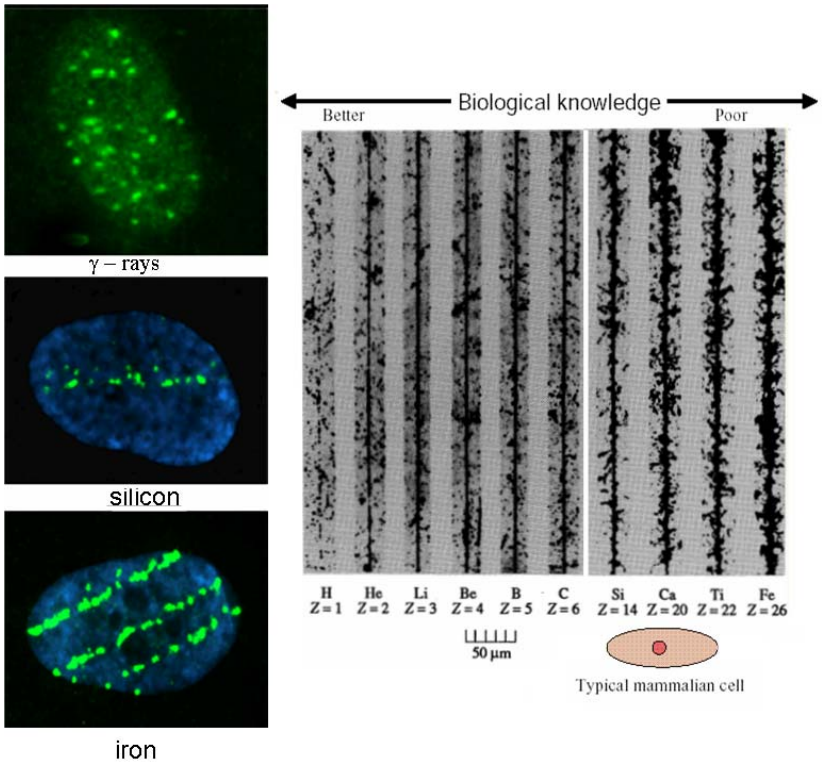

Figure 4-3. ***Comparison of particle tracks in nuclear emulsions and human cells (Cucinotta and Durante, 2006). The right panel shows tracks of different ions, from protons to Fe, in nuclear emulsions, clearly showing the increasing ionization density (LET=ΔE/Δ x) along the track by increasing the charge Z. The left panel shows three nuclei of human fibroblasts exposed to gamma rays or to Si- or Fe-ions, and immunostained for detection of γ-H2AXP. Each green focus corresponds to a DNA double strand break (DSB). While in the cell that is exposed to sparsely ionizing gamma rays foci of the histone variant, H2AX, are uniformly distributed in the nucleus, the cells that are exposed to HZE particles present DNA damage along tracks (one Si- and three Fe-particles, respectively), and the spacing between DNA DSB is reduced at a very high LET.***

HZE nuclei impart damage via the primary energetic particle as well as from fragmentation events that produce a spectrum of other energetic nuclei, including protons, neutrons, and heavy fragments (Wilson et al., 1995; Cucinotta et al., 1998a; 2006); a large penumbra of energy deposition extends outward from the primary particle

track (Cucinotta et al., 2000a). Secondary radiation that is produced in shielding materials can be controlled through the use of materials that have light atomic constituents (e.g., hydrogen and carbon). However, a large percentage of secondary radiation is produced within tissue and is, therefore, not practically avoidable. Due to the large amount of energy that is deposited as these particles traverse biological structures, the HZE nuclei are capable of producing the greatest amount of cellular damage, which means that they are of great concern for astronaut safety. The lack of epidemiological data and sparse radiobiological data on the effects for these radiation types leads to a high level of uncertainty when formulating risk estimates of long-term health effects following exposure to GCRs and SPEs.

Types of cancer caused by radiation exposure

A broad spectrum of tissue types contributes to the overall cancer risk that is observed with low-LET radiation (Table 4-2), including lung, colorectal, breast, stomach, liver, and bladder cancers as well as several types of leukemia, including acute myeloid leukemia and acute lymphatic lymphoma (NCRP, 2000; Preston et al., 2003; BEIR, 2006). It is not known whether the same spectrum of tumors will occur for high-LET radiation as with low-LET radiation, and some differences should be expected. Relative biological effectiveness (RBE) factors describe the ratio of a dose of high-LET radiation to that of the X rays or gamma rays that produce the identical biological effect. RBEs that are observed in mice with neutrons vary with the tissue type and strain of the animal (NCRP, 1990; Fry and Storer, 1987), which provides evidence that the spectrum of tumors in humans who are exposed to space radiation will be distinct from that in humans who are exposed to low-LET radiation. These likely differences are not described by the models that are used currently at NASA to project space radiation risks.

Age, latency, gender, and individual sensitivity issues

As cancer is a genetic disease with important epigenetic factors, individual susceptibility issues are an important consideration for space radiation protection. Females have a higher cancer risk from radiation than males, largely due to the additional risks to the breast and ovary; but studies show that there is also a much higher risk of lung cancer after radiation exposure in females than in males (NCRP, 2000). Risk at a sufficiently high age would be expected to decrease with age at exposure because the distribution of latency for tumor development would extend beyond the expected life span at older exposure ages. There may also be a reduction in the number of cells that are at risk at older age due to senescence or other biological factors (Campisi, 2003; 2007). However, the possibility that radiation acts more as a tumor promoter than as an initiator, and the fact that the animal data for high-LET radiation show tumors developing at earlier times than with low-LET radiation, suggests that the age dependence of space cancer risk is inadequately understood at this time.

Genetic factors and environmental factors also impact the risk of cancer from radiation. Studying the mechanisms of genetic sensitivity provides important insights into the understanding of radiation risks to astronauts (Durante and Cucinotta, 2008). Studies of historical data sets, such as the atomic-bomb survivors, show that subsets of the exposed cohorts could have a higher-than-average radiation risk (Ponder, 2001). A well-known example is *ataxia telangiectasia* (AT) patients, who dramatically demonstrate the importance of genetic susceptibility to radiation damage in cancer treatment. Other examples that are related to DNA repair genes include BRCA1&2 (Ponder, 2001, p. 53), NBS (Pluth et al., 2008), and Artemis (Wang et al., 2005), as well as the many other so-called high-penetrance genes that are involved in cancer susceptibility (Ponder, 2001).

Ataxia telangiectasia mutated (ATM) homozygotes only represent a small fraction of the radiosensitive patients, although these patients appear to be the most sensitive. ATM heterozygotes, who are also cancer-prone, are suspected to represent a large fraction of the extreme radiosensitive patients (Thompson et al., 2005).

It has been shown that cells that are heterozygous for ATM mutations are slightly more sensitive to radiation-induced neoplastic transformation than are the wild-type cells (Sminelov et al., 2001). An increased sensitivity of ATM heterozygotes has been also proved in vivo, measuring the induction of cataracts in ATM homozygotes, heterozygotes, and wild-type mice exposed to 0.5- to 4-Gy X rays (Worgul et al., 2002).

An important issue to address is how low-penetrance genes impact sensitivity to radiation-induced cancer. A recent study on subjects who were exposed to high radiation doses to treat ringworm of the scalp (*tinea capitis*) in Israel revealed a strong familial risk of radiation-induced meningioma (Flint-Ritcher and Sadetzki, 2007), suggesting that radiation carcinogenesis might be an issue for a genetically predisposed subgroup of the general population rather than a random event (Hall, 2007).

It is not known whether individuals who display hypersensitivity to low-LET radiation will also be equivalently hypersensitive to HZE nuclei, or whether findings at high dose and dose-rates will hold at low dose-rates and doses. Mice that are heterozygous for the ATM gene are more sensitive to cataractogenesis than are wild-types, not only after exposure to X rays but also after localized irradiation with high-energy Fe-ions (Hall et al., 2006). However, other studies show that high-LET irradiation has a reduced dependence on genetic background compared to low-LET irradiation (George et al., 2009).

A predictive assay that is able to identify radiation hypersensitive or cancer-prone subjects could be useful in crew selection for long-term space flights. Alternatively, identifying resistant individuals could substantially lower mission costs. Although this assay is neither scientifically achievable nor within society norms in most countries at the present time, ultimately, for a high-risk and high-cost endeavor such as a mission to Mars, screening astronauts for increased resistance to space radiation may be sought to reduce the costs of the missions.

Current NASA permissible exposure limits

Permissible exposure limits (PELs) for short-term and career astronaut exposures to space radiation have been approved by the NASA Chief Health and Medical Officer, and requirements and standards for mission design and crew selection have been set. This section describes the cancer risk section of the PELs.

Career Cancer Risk Limits

The astronaut career exposure to radiation is limited to not exceed 3% of the risk of exposure-induced death (REID) from fatal cancer. NASA policy is to assure that this risk limit is not exceeded at a 95% confidence level (CL) by using a statistical assessment of the uncertainties in the risk projection calculations to limit the cumulative effective dose (in units of Sievert) that is received by an astronaut throughout his or her career. These limits are applicable to missions of any duration in LEO and to lunar missions of less than 180 days duration. For longer missions that are outside LEO, further considerations of non-cancer mortality risks and approaches to reduce uncertainty in cancer risk projection models must occur before these missions can be safely assured.

Cancer Risk to Dose Relationship

The relationship between radiation exposure and risk is both age- and gender-specific due to latency effects and differences in tissue types, sensitivities, and life spans between genders. These relationships are estimated using the methods that are recommended by the NCRP (NCRP, 2000) and more recent radiation epidemiology information (Preston et al., 2003; Cucinotta et al., 2006). Table 4-1 lists examples of career effective dose (E) limits for an REID=3% for missions that are of 1-year duration or less. Limits for other career or mission lengths will vary and should be calculated using the appropriate life-table formalism. Tissue contributions to effective doses are defined below, as are dose limits for other career or mission lengths. Estimates of average life-loss

that are based on low-LET radiation are also listed in Table 4-1; however, higher values should be expected for high-LET exposures such as GCRs.

Table 4-1. ***Example Career Effective Dose Limits in Units of milli-Sievert (mSv) for 1-year Missions and Average Life-loss for an Exposure-induced Death for Radiation Carcinogensis (1 mSv = 0.1 rem)***

	E(mSv) for 3% REID (Ave. Life Loss per Death, yr)	
Age, yr	**Males**	**Females**
25	520 (15.7)	370 (15.9)
30	620 (15.4)	470 (15.7)
35	720 (15.0)	550 (15.3)
40	800 (14.2)	620 (14.7)
45	950 (13.5)	750 (14.0)
50	1,150 (12.5)	920 (13.2)
55	1,470 (11.5)	1,120 (12.2)

The Principle of As Low As Reasonably Achievable

The as low as reasonably achievable (ALARA) principle is a legal requirement intended to ensure astronaut safety. An important function of ALARA is to ensure that astronauts do not approach radiation limits and that such limits are not considered as "tolerance values." ALARA is especially important for space missions in view of the large uncertainties in cancer and other risk projection models. Mission programs and terrestrial occupational procedures resulting in radiation exposures to astronauts are required to find cost-effective approaches to implement ALARA.

Method of evaluating career limits

Radiation Doses and Risk Limits

Cancer risk is not measured directly but is calculated using radiation dosimetry and physics methods. The absorbed dose D (in units of Gray) is calculated using measurements of radiation levels that are provided by dosimeters (e.g., film badges, thermoluminescent dosimeters (TLDs), spectrometers such as the tissue-equivalent proportional counter (TEPC), area radiation monitors, biodosimetry, or biological markers) and corrections for instrument limitations. The limiting risk is calculated using the effective dose, *E* (in units of mSv), and risk conversion life-table methodologies.

For the purpose of determining radiation exposure limits at NASA, the probability of fatal cancer is calculated as shown on the following page.

1. The body is divided into a set of sensitive tissues, and each tissue, T, is assigned a weight, w_T, according to its estimated contribution to cancer risk, as shown in Table 4-2.

Table 4-2. *Tissue Weighting Factors*

Tissue or Organ	Tissue Weighting Factor, w_T
Gonads	0.20
Bone Marrow (red)	0.12
Colon	0.12
Lung	0.12
Stomach	0.12
Bladder	0.05
Breast	0.05
Liver	0.05
Esophagus	0.05
Thyroid	0.05
Skin	0.01
Bone Surface	0.01
Remainder*	0.05

*For purpose of calculation, the remainder is composed of the following additional tissues and organs: adrenals, brain, upper intestine, small intestine, kidney, muscle, pancreas, spleen, thymus, and uterus.

2. The absorbed dose, D_T, that is delivered to each tissue is determined from measured dosimetry. Different types of radiation have different biological effectiveness, depending on the ionization density that is left behind locally (e.g., in a cell or a cell nucleus) by the passage of radiation through matter. For the purpose of estimating radiation risk to an organ, the quantity characterizing this ionization density is the LET (in units of keV/μm).

3. For a given interval of LET, between L and ΔL, the dose-equivalent risk (in units of Sievert, where 1 Sv = 100 rem) to a tissue, T, $H_T(L)$ is calculated as

$$H_T(L) = Q(L)D_T(L), \tag{1}$$

where the quality factor, $Q(L)$, is obtained according to the International Commission on Radiation Protection (ICRP) prescription that is shown in Table 4-3. This way of calculating $H_T(L)$ differs from the method that is used by the ICRP, in which a tabulated set of weighting factors is given instead of the quality factor. The method that is used here is considered to yield a better approximation by using the quality factor as the weight that is most representative of cancer risk; the ICRP method, by contrast, may overestimate the risk, especially for high-energy protons. Neutron contributions are evaluated by their contribution to $D_T(L)$.

Table 4-3. *Quality Factor – Linear Energy Transfer Relationship*

Unrestricted LET, keV/μm in Water	Q(LET)
<10	1
10 to 100	0.32 LET – 2.2
>100	300/ Sqrt(LET)

4. The average risk to a tissue T, due to all types of radiation contributing to the dose, is given by

$$H_T = \int D_T(L)Q(L)dL, \tag{2}$$

or, since $D_T(L) = LF_T(L)$, where $F_T(L)$ is the fluence of particles with LET=L, traversing the organ,

$$H_T = \int dLQ(L)F_T(L)L. \tag{3}$$

5. The effective dose is used as a summation over radiation type and tissue using the tissue weighting factors, w_T,

$$E = \sum_T w_T H_T. \quad (4)$$

6. For a mission of duration t, the effective dose will be a function of time, $E(t)$, and the effective dose for mission i will be

$$E_i = \int E(t)dt. \quad (5)$$

7. The effective dose is used to scale the mortality rate for radiation-induced death from the Japanese survivor data, applying the average of the multiplicative and additive transfer models for solid cancers and the additive transfer model for leukemia by applying life-table methodologies that are based on U.S. population data for background cancer and all causes of death mortality rates. A DDREF of 2 is assumed.

Evaluation of Cumulative Radiation Risks

The cumulative cancer fatality risk (%REID) to an astronaut for occupational radiation exposures, N, is found by applying life-table methodologies that can be approximated at small values of %REID by summing over the tissue-weighted effective dose, E_i, as

$$Risk = \sum_{i=1}^{N} E_i R_0(age_i, gender), \quad (6)$$

where R_0 are the age- and gender-specific radiation mortality rates per unit dose. The effective dose limits that are given in the Table 4-1 illustrate the effective dose that corresponds to a 3% REID for missions with a duration of as long as 1 year. Values for multiple missions or other occupational exposure are estimated using Eq(6) or directly from life-table calculations. For organ dose calculations, NASA uses the model of Billings et al. (1973) to represent the self-shielding of the human body in a water-equivalent mass approximation. Consideration of the orientation of the human body relative to vehicle shielding should be made if it is known, especially for SPEs (Wilson et al., 1995).

Confidence levels for career cancer risks are evaluated using methods that are specified by the NCRP in Report No. 126 (NCRP, 1997a), which was modified to account for the uncertainty in quality factors and space dosimetry (Cucinotta et al., 2001; 2006). The uncertainties that were considered in evaluating the 95% CLs are the uncertainties in

1. Human epidemiology data, including uncertainties in

   a. statistics limitations of epidemiology data,
   b. dosimetry of exposed cohorts,
   c. bias, including misclassification of cancer deaths, and
   d. the transfer of risk across populations.

2. The DDREF factor that is used to scale acute radiation exposure data to low-dose and dose-rate radiation exposures.

3. The radiation quality factor (Q) as a function of LET.

4. Space dosimetry.

The so-called "unknown uncertainties" from the NCRP Report No. 126 (1997a) are ignored by NASA. The statistical distribution for the estimated probability of fatal cancer is evaluated to project the most likely values and the lower and upper 95% C.I.'s that are reported within brackets. For example, for the average adult who is exposed to 100 mSv (10 rem) of gamma rays, the estimated cancer risk is 0.4 % and the 95%. C.I.'s are estimated as [0.11%, 0.82%] where 0.11% is the lower 95% level and 0.82% is the upper 95% CL. To assure that the career risk limit is not exceeded with a safety margin corresponding to a 95% CL, the upper CL (i.e., the worse case) is considered in developing mission constraints and for crew selection. Approximate fold-uncertainties for several NASA missions are shown in Table 4-4.

Table 4-4. ***Approximate Fold-uncertainty Defined as a Ratio of Upper 95% Confidence Level to Point Risk Projection***

Type of Exposure	Fold-uncertainty at Upper 95% C.I.
Medical Diagnostic	2.0
ISS Environment	3.1
SPE	2.5
Deep Space or Lunar Surface GCR	4.0

Evidence

The evidence and updates to projection models for cancer risk from low-LET radiation are reviewed periodically by several prestigious bodies, which include the following organizations:

- The NAS Committee on the Biological Effects of Ionizing Radiation
- The United Nations Scientific Committee on the Effects of Atomic Radiation (UNSCEAR)
- The ICRP
- The NCRP

These committees release new reports about every 10 years on cancer risks that are applicable to low-LET radiation exposures. Overall, the estimates of cancer risks among the different reports of these panels will agree to within a factor of two or less. There is continued controversy for doses that are below 50 mSv, however, and for low dose-rate radiation because of debate over the linear no-threshold hypothesis that is often used in statistical analyses of these data. The BEIR VII report (BEIR, 2006), which is the most recent of the major reports, is used in the following summary. Evidence for low-LET cancer effects must be augmented by information on protons, neutrons, and HZE nuclei that is only available in experimental models. Such data have been reviewed by NASA several times in the past and by the NCRP (1989; 2000; 2006).

Epidemiology data for low-linear energy transfer radiation

Life Span Studies of Atomic Bomb Survivors

The life span study (LSS) of the survivors of the atomic bombs in Hiroshima and Nagasaki, Japan, includes approximately 130,000 persons who were registered in 1950. Among these were 93,000 persons in Hiroshima and Nagasaki in 1945, and 37,000 persons who were living in these same cities in 1950. There is a gap in knowledge of the earliest cancer that developed in the first few years after the war, which impacts the assessment of leukemia to an important extent and for solid cancers to a minor extent. Some of the persons in the total data set were censured, leading to about 86,000 persons who have been followed in the study. Table 4-5 shows summary statistics of the number of persons and deaths for different dose groups. These comparisons show that the doses that were received by the LSS population overlap strongly with the doses that are of concern to NASA Exploration mission (i.e., 50 to 2,000 mSv).

Figure 4-4 shows the dose response for the excess relative risk (ERR) for all solid cancers from Preston et al. (2003). Tables 4-6 and 4-7 show several summary parameters for tissue-specific cancer mortality risks for females and males, respectively, including estimates of ERR, excess absolute risk (EAR), and percentage attributable risks. Cancer incidence risks from low-LET radiation are about 60% higher than cancer mortality risks (Preston et al., 2007).

Table 4-5. Number of Persons, Cancer Deaths, and Non-cancer Deaths for Different Dose Groups in the Life Span Study (BEIR, 2006)

	DS86 Weighted Colon Dose, mSv							
	Total	**0-50**	**50–100**	**100–200**	**200–500**	**500–1,000**	**1,000–2,000**	**>2,000**
No. Subjects	86,572	37,458	31,650	5,732	6,332	3,299	1,613	488
Cancer Deaths	9,335	3,833	3,277	668	763	438	274	82
Non-cancer Deaths	31,881	13,832	11,633	2,163	2,423	1,161	506	163

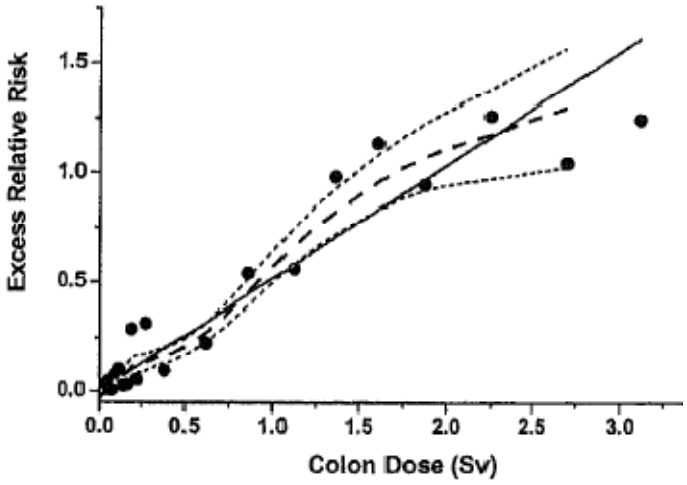

Figure 4-4. ***From Preston et al. (2003): Solid cancer dose-response function average over sex for attained age 70 after exposure at age 30. The solid straight-line is the linear slope estimate; the points are dose-category-specific ERR estimates; the dashed curve is a smoothed estimate that is derived from the points; and the dotted curves indicate upper and lower one-stand-error bounds on the smoothed estimate.***

Table 4-6. ***From Preston et al. (2003): Tissue-specific Cancer Mortality Risk Summary Statistics (i.e., ERR, EAR, and Attributable Risks) for Females and Males, Respectively***

LSS Female Site-specific Summary Mortality Rate Estimates: Solid Cancers 1950–1997

Site/system	Deaths (>0.005 Sv)	ERR/Sv[a] (90% CI)	EAR/10^4PY[b]-Sv[c] (90% CI)	Attributable risk (%)[d] (90% CI)
All solid cancer	4,884 (2,948)	0.63 (0.49; 0.79)	13.5 (7.4; 16.3)	9.2 (7.4; 11.0)
Oral cavity	42 (25)	–0.20 (<–0.3; 0.75)	–0.04 (<–0.3; 0.14)	–4.1 (<–6; 14)
Digestive system				
Esophagus	67(44)	1.7 (0.46; 3.8)	0.51 (0.15; 0.92)	22 (6.6; 42)
Stomach	1,312 (786)	0.65 (0.40; 0.95)	3.3 (2.1; 4.7)	8.8 (5.5; 12)
Colon	272 (150)	0.49 (0.11; 1.1)	0.68 (0.76; 1.3)	9.0 (3.4; 17)
Rectum	198 (127)	0.75 (0.16; 1.6)	0.69 (0.16; 1.3)	11.3 (2.6; 22)
Liver	514 (291)	0.35 (0.07; 0.72)	0.85 (0.18; 1.6)	6.2 (1.3; 12)
Gallbladder	236 (149)	0.16 (–0.17; 0.67)	0.18 (–0.21; 0.71)	2.6 (–2.9; 10)
Pancreas	244 (135)	–0.01 (–0.28; 0.45)	–0.01 (–0.35; 0.52)	–0.2 (–5.0; 7.6)
Respiratory system				
Lung	548 (348)	1.1 (0.678; 1.6)	2.5 (1.6; 3.5	16 (10; 22)
Female breast	272 (173)	0.79 (0.29; 1.5)	1.6 (1.2; 2.2)	24 (18; 32)
Uterus	518 (323)	0.17 (–0.10; 0.52)	0.44 (–0.27; 1.3)	2.7 (–1.6; 7.9)
Ovary	136 (85)	0.94 (0.07; 2.0)	0.63 (0.23; 1.2)	15 (5.3; 28)
Urinary system				
Bladder	67 (43)	1.2 (0.10; 3.1)	0.33 (0.02; 0.74)	16 (0.9; 36)
Kidney	31 (21)	0.97 (<–0.3; 3.8)	0.14 (<–0.1; 0.42)	14 (<–3; 42)
Brain/CNS[d]	17 (10)	0.51 (<–0.3; 3.9)	0.04 (<–0.02; 0.2)	11 (<0.05; 57)

[a]ERR/SV for age at exposure 30 in an age-constant linear ERR model; [b]Excess absolute risk per 10,000 persons per year; [c]Average EAR computed from ERR model; [d]Attributable risk among survivors whose estimated dose is at least 0.005 Sv; CNS – central nervous system.

Table 4-7. ***From Preston et al. (2003): Tissue-specific Cancer Mortality Risk Summary Statistics (i.e., ERR, EAR, and Attributable Risks) for Male***

LSS Male Site-specific Summary Mortality Rate Estimates: Solid Cancers 1950–1997

Site/system	Deaths (>0.005 Sv)	ERR/Sv[a] (90% CI)	EAR/10^4PY[b]-Sv[c] (90% CI)	Attributable risk (%)[d] (90% CI)
All solid cancer	4,451 (2,554)	0.37 (0.26; 0.49)	12.6 (9.4; 16.2)	6.6 (4.9; 8.4)
Oral cavity	68 (37)	–0.20 (<–0.3; 0.45)	–0.12 (<–0.3; 0.25)	–5.2 (<–6; 11)
Digestive system				
Esophagus	224 (130	0.61 (0.15; 1.2)	1.1 (0.28; 2.0)	11.1 (2.8; 21)
Stomach	1,555 (899)	0.20 (0.04; 0.39)	2.1 (0.43; 4.0)	3.2 (0.07; 6.2)
Colon	206 (122)	0.54 (0.13; 1.2)	1.1 (0.64; 1.9)	12 (6.9; 21)
Rectum	172 (96)	–0.25 (<–0.3; 0.15)	–0.41 (<–0.4; 0.22)	–5.4 (<–6, 3.1)
Liver	722 (408)	0.59 (0.11; 0.68)	2.4 (1.2; 4.0)	8.4 (4.2; 14)
Gallbladder	92 (52)	0.89 (0.22; 1.9)	0.63 (0.17; 1.2)	17 (4.5; 33)
Pancreas	163 (103)	–0.11 (<–0.3; 0.44)	–0.15 (<–0.4; 0.58)	–1.9 (<–6; 7.5)
Respiratory system				
Lung	716 (406)	0.48 (0.23; 0.78)	2.7 (1.4; 4.1)	9.7 (4.9; 15)
Prostate	104(53)	0.21 (<–0.3; 0.96)	0.18 (<–0.2; 0.75)	4.9 (<–5; 20)
Urinary system				
Bladder	82 (56)	1.1 (0.2; 2.5)	0.7 (0.1; 1.4)	17 (3.3; 34)
Kidney	36 (18)	–0.02 (<–0.3; 1.1)	–0.01 (–0.1; 0.28)	–0.4 (<–5; 22)
Brain/CNS	14 (9)	5.3 (1.4; 16)	0.35 (0.13; 0.59)	62 (23; 100)

[a]ERR/SV for age at exposure 30 in an age-constant linear ERR model; [b]Excess absolute risk per 10,000 persons per year; [c]Average EAR computed from ERR model; [d]Attributable risk among survivors whose estimated dose is at least 0.005 Sv.

Other Human Studies

The BEIR VII report (BEIR, 2006) contains an extensive review of data sets from human populations, including nuclear reactor workers and patients who were treated with radiation. The recent report from Cardis et al. (2007) describes a meta-analysis for reactor workers from several countries. A meta-analysis at specific cancer sites, including breast, lung, and leukemia, has also been performed (BEIR, 2006). These studies require adjustments for photon energy, dose-rate, and country of origin as well as adjustments made in single population studies. Table 4-8 shows the results that are derived from Preston et al. (2002) for a meta-analysis of breast cancer risks in eight populations, including the atomic-bomb survivors. Median ERR varies by slightly more than a factor of two, but confidence levels significantly overlap. Adjustments for photon energy or dose-rate and fractionation have not been made. These types of analysis lend confidence to risk assessments as well as show the limitations of such data sets.

Of special interest to NASA is the age at exposure dependence of low-LET cancer risk projections. The BEIR VII report (BEIR, 2006) prefers models that show less than a 25% reduction in risk over the range from 35 to 55 years, while NCRP Report No. 132 (NCRP, 2000) shows about a two-fold reduction over this range.

Table 4-8. ***Results from Meta-analysis of Breast Cancer Risk from Eight Population Groups, Including the Life Span Study of Atomic-bomb Survivors and Several Medical Patient Groups Exposed to X Rays, as described in Preston et al., 2002***

Summary of Parameter Estimates for the Final Pooled ERR Model

Cohort	Reference age for the ERR/Gy estimate	ERR/Gy[a]	Percentage change per decade increase in age at exposure	Exponent of attained age	Background SIR[b]
LSS	attained age 50	2.10 (1.6; 2.8)	Not included[b]	–2.0 (–2.8; –1.1)	1.01 (0.9; 1.1)
TBO	attained age 50	0.74 (0.4; 1.2)	Not included	–2.0 (–2.8; –1.1)	0.96 (0.7; 1.2)
TBX	attained age 50	0.74 (0.4; 1.2)	Not included	–2.0 (–2.8; –1.1)	0.73 (0.6; 0.9)
THY	attained age 50	0.74 (0.4; 1.2)	Not included	–2.0 (–2.8; –1.1)	1.05 (0.7; 1.5)
BBD	age at exposure 25	1.9 (1.3; 2.8)	–60% (–71%; –44%)	Not included[c]	0.98 (0.8; 1.2)
APM	all ages	0.56 (0.3; 0.9)	Not included	Not included	1.45 (1.1; 1.8)
HMG	all ages	0.34 (0.1; 0.7)	Not included	Not included	1.07 (0.8; 1.3)
HMS	all ages	0.34 (0.1; 0.7)	Not included	Not included	1.05 (0.9; 1.2)

[a]95% C.I.'s within parentheses; [b]SIR = standardized incidence ratio; [c]"Not included" means that the risk is assumed not to vary with age at exposure (attained age).

Review of space flight issues

In considering radiation risks for astronauts, it is useful to consider the historical recommendations that NASA has received from external advisory committees. These have formed the basis for the dose limits and risk projection models (Cucinotta et al., 2002). Early radiation effects usually are related to a significant fraction of cell loss that exceeds the threshold for impairment of function in a tissue. These "deterministic" effects are so called because the statistical fluctuations in the number of affected cells are very small compared to the number

of cells that are required to reach the threshold (ICRP, 1991). Maintaining dose limits can ensure that no early effects occur; these are expected to be accurately understood. As late effects can result from changes in a very small number of cells, statistical fluctuations can be large and some level of risk is incurred even at low doses. Referring to them as "stochastic" effects recognizes the predominance of statistical effects in their manifestation.

In recommendations by the NAS in 1967 (NRC, 1967), it was noted that radiation protection in human space flight is philosophically distinct from the protection practices of terrestrial workers because of the high-risk nature of space missions. This report by the NAS from 1967 did not recommend "permissible doses" for space operations, noting the possibility that such limits may jeopardize the mission, but instead estimated what the likely effects would be for a given dose of radiation.

In 1970, the NAS Space Science Board (NRC, 1970) recommended guidelines for career doses to be used by NASA for long-term mission design and human operations. At that time, NASA employed only male astronauts and the typical age of astronauts was 30 to 40 years. A "primary reference risk" was proposed that was equal to the natural probability of cancer over a period of 20 years following the radiation exposure (using the period from 35 to 55 years of age); this was essentially a doubling dose. The estimated doubling dose of 382 rem (3.82 Sv), which ignored a dose-rate reduction factor, was rounded to 400 rem (4 Sv). The NAS panel noted that its recommendations were not risk limits but, rather, a reference risk, and that a higher risk could be considered for planetary missions or a lower level of risk for a possible space station mission (NRC, 1970). Ancillary reference risks were described to consider monthly, annual, and career exposure patterns. However, the NAS recommendations were implemented by NASA as dose limits that were used operationally for all missions until 1989.

At the time of the 1970 NAS report, the major risk from radiation was believed to be leukemia. Since that time, the maturation of the data from the Japanese atomic-bomb survivors has led to estimates of higher levels of cancer risk for a given dose of radiation, including the observation that the risk of solid tumors following radiation exposure occurs with a higher probability than that of leukemias, although with a longer latency period before expression. Figure 4-5 illustrates the changing estimates of cancer risks for an average adult worker since 1970. Together with the maturation of the atomic-bomb data, reevaluation of the dosimetry of the atomic-bomb survivors, scientific assessments of the dose response models, and dose-rate dependencies have contributed to the large increase in risk estimate over this time period (1970–1997). The possibility of future changes in risk estimates can, of course, not be safely predicted today; it is possible that such changes could potentially impact NASA mission operations. Thus, protection against uncertainties is an ancillary condition to the ALARA principle, suggesting that conservatism be exercised as workers approach dose limits.

By the early 1980s, several major changes had occurred that led to the need for a new approach in defining dose limits for astronauts. At that time, NASA requested that the NCRP reevaluate the dose limits that were to be used for LEO operations. Considerations included the increases in estimates of radiation-induced cancer risks, the criteria for risk limits, and the role of the evolving makeup of the astronaut population from male test pilots to a larger, diverse population of astronauts (~100), including mission specialists, female astronauts, and career astronauts of higher ages who often participate in several missions. In 1989, NCRP Report No. 98 (NCRP, 1998) recommended age- and gender-dependent career dose limits using a 3% increase in cancer mortality as a common risk limit. This limiting level of 3% excess cancer fatality risk was based on several criteria, including a comparison to dose limits for ground radiation workers and to rates of occupational death in less-safe industries. It was noted that astronauts face many other risks, and that an overly large radiation risk was not justified. It also should be noted that the average years of life loss from radiation-induced cancer death, which is about 15 years for workers over age 40 years and 20 years for workers between age 20 and 40 years, is less than that of other occupational injuries. A comparison of radiation-induced cancer deaths to cancer fatalities in the U.S.

population is also complex because of the smaller years of life loss in the general population, where most cancer deaths occur above age 70 years.

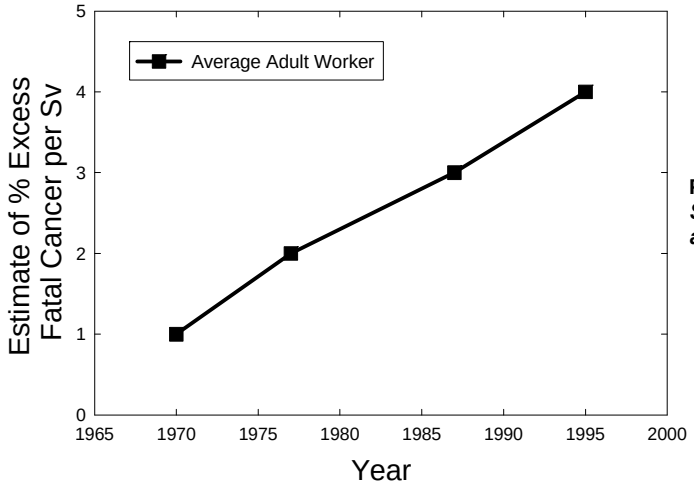

Figure 4-5. ***Estimates of the risk per Sv delivered at low dose-rates for the average adult worker from 1970 to 1997.***

In the 1990s, the additional follow-up and evaluation of atomic-bomb survivor data led to further increases in the estimated cancer risk for a given dose of radiation. Recommendations from the NCRP (NCRP, 2000), while keeping the basic philosophy of risk limitation that had been in the earlier report, advocate significantly lower limits than those that were recommended in 1989 (NCRP, 1989). Table 4-9 provides examples of career radiation limits for a career duration of 10 years, with the doses assumed to be spread evenly over the career. The values from the previous report are also listed for comparison. Both of these reports specify that these limits do not apply to Exploration missions because of the large uncertainties in predicting the risks of late effects from heavy ions.

Table 4-9. ***Career Dose Limits (in Sv) Corresponding to a 3% Excess Cancer Mortality for 10-year Careers as a Function of Age and Sex, as Recommended by the NCRP (NCRP, 1989; 2000)***

Age, year	NCRP Report No. 98		NCRP Report No. 132	
	Male (Sv)	Female (Sv)	Male (Sv)	Female (Sv)
25	1.5	1.00	0.7	0.4
35	2.5	1.75	1.0	0.6
45	3.2	2.50	1.5	0.9
55	4.0	3.00	3.0	1.7

The NCRP Report No. 132 (NCRP, 2000) notes that the use of comparisons to fatalities in the less-safe industries that were advocated by the NCRP in 1989 were no longer viable because of the large improvements that had been made in ground-based occupational safety. Table 4-10, which shows an update to such a comparison, demonstrates that, indeed, the decreased rate of fatalities in the so-called less safe industries (e.g., mining, agriculture) would suggest a limit below the 3% fatality level today as compared to that in 1989. The most recent reviews of the acceptable levels of radiation risk for LEO, including that provided during a 1996 NCPR symposium (NCRP, 1997b) and the recent NCRP Report No. 132 on the LEO dose limits (NCRP, 2000), instead advocate that comparisons to career dose limits for ground-based workers be used. It is also widely

held that the social and scientific benefits of space flight continue to provide justification for the 3% risk level for astronauts who are participating in LEO missions.

In comparison to the limits that have been set by NASA, the U.S. nuclear industry uses age-specific limits that are gender-averaged, which is of sufficient accuracy for the low doses received by nuclear workers. Here career limits are set at a total dose-equivalent that is equal to the individual's age × 0.01 Sv. It is estimated by the NCRP that ground workers who reach their dose limits would have a lifetime risk of about 3%, but note the difference in dose values corresponding to the limit is due to differences in how the radiation doses are accumulated over the worker's career. The short-term (30-day and 1-year) dose limits set by NASA are several times higher than those of terrestrial workers because they are intended to prevent acute risks, while the annual dose limits of 50 mSv (5 rem), which are followed by U.S. terrestrial radiation workers, control the accumulation of career doses.

Table 4-10. ***Occupational Death Rates (National Safety Council) and Lifetime Risks for 40-year Careers for the Less-safe and Safe Industries***

Occupation	Deaths per 10,000 Workers per year			Lifetime Risk (%) of Occupational Death		
	1977	1987	2002	1977	1987	2002
Agriculture	5.4	4.9	2.1	2.2	2.0	0.8
Mining	6.3	3.8	2.9	2.5	1.5	1.2
Construction	5.7	3.5	1.3	2.3	1.4	0.6
Transportation	3.1	2.8	1.0	1.2	1.1	0.5
Manufacturing	0.9	0.6	0.28	0.4	0.2	0.1
Government	1.1	0.8	0.26	0.4	0.3	0.1
All	1.4	1.0	0.36	0.6	0.4	0.2

The exposures that are received by radiation workers in reactors, accelerators, hospitals, etc. rarely approach dose limits with the average annual exposure of 1 to 2 mSv, which is a factor of 25 below the annual exposure limit and significantly less than the average dose for a 6-month ISS mission (100 mSv). Similarly, transcontinental pilots, although they are not characterized as radiation workers in the U.S., receive an annual exposure of about 1 to 5 mSv, and enjoy long careers without approaching the exposure limits that are recommended for terrestrial workers in the U.S. Under these conditions, ground-based radiation workers are estimated to be well below the career limits, even if a 95% CL is applied. As space missions have been of relatively short duration in the past, thereby requiring minimal mitigation, the impact of dose limits when space programs actually approach such boundaries, including the application of the ALARA principle, has been unexplored.

Summary of Approaches for Setting Acceptable Levels of Risk

The various approaches to setting acceptable levels of radiation risk are summarized below.

1. *Unlimited Radiation Risk:* NASA management, the families or loved ones of astronauts, and taxpayers would find this approach unacceptable.

2. *Comparison to Occupational Fatalities in Less-safe Industries*: The life-loss from attributable radiation cancer death is less than that from most other occupational deaths. At this time, this comparison would also be very restrictive on ISS operations because of continued improvements in ground-based occupational safety over the last 20 years.

3. *Comparison to Cancer Rates in General Population:* The number of years of life-loss from radiation-induced cancer deaths can be significantly larger than from cancer deaths in the general population, which often occur late in life (>age 70 years) and with significantly less numbers of years of life-loss.

4. *Doubling Dose for 20 Years Following Exposure:* Provides a roughly equivalent comparison based on life-loss from other occupational risks or background cancer fatalities during a worker's career; however, this approach negates the role of mortality effects later in life.

5. *Use of Ground-based Worker Limits:* Provides a reference point equivalent to the standard that is set on Earth, and recognizes that astronauts face other risks. However, ground workers remain well below dose limits, and are largely exposed to low-LET radiation where the uncertainties of biological effects are much smaller than for space radiation.

A more recent review of cancer and other radiation risks is provided by the NCRP Report No.153 (NCRP, 2006). The stated purpose of this report is to identify and describe the information that is needed to make radiation protection recommendations for space missions beyond LEO. The report contains a comprehensive summary of the current body of evidence for radiation-induced health risks, and makes recommendations on areas requiring future experimentation.

Past space missions

The radiation doses on past space missions have been well characterized using physical and biological dosimetry and radiation transport models (Cucinotta et al., 2001; 2003a; 2008). Phantom torso experiments have been performed on ISS and space shuttle (Badhwar et al., 2000; Yasuda et al., 2000; Cucinotta et al., 2008). Phantom torsos offer good evidence of the accuracy of the NASA radiation transport code, HZETRN (Wilson et al., 1995), nuclear interaction cross sections (Cucinotta et al., 2006). Organ dose and dose-equivalent predictions are shown to agree with measurements to within ±15% in most cases, as shown in Table 4-11(a) and (b) (Cucinotta et al., 2008).

Biodosimetry, which has been performed on all ISS missions as well as for four astronauts on *Mir* missions, offers an alternative evaluation of organ dose-equivalents. Figure 4-6 shows results for the pre- and post-flight frequency of translocations, which are complex aberrations involving more than two chromosomes, and total exchanges. Total exchanges are increased post-flight over pre-flight values in all cases, and translocations increase in all ISS astronauts, but they did not increase for two astronauts: one who was returning from the *Mir* space station, and one who was on a Hubble repair mission. To test whether the overall frequency of complex aberrations was increased by space radiation, Cucinotta et al. (2008) pooled results into two groups: all ISS data, and all ISS data plus results from other NASA missions. The relative frequencies for complex aberrations and translocations were shown to be highly significant ($P<10^{-4}$) (Cucinotta et al., 2008).

Figure 4-7 shows a summary of the crew doses for all NASA missions through the year 2007. The level of accuracy in effective dose determination and in the GCR environments suggests a high level of accuracy in predicting organ dose and dose-equivalencies for both lunar and Mars missions. The cancer projection model of NCRP Report No. 132 (NCRP, 2000), which can be applied to these effective doses, indicates REID values approaching 1% for many astronauts who have flown on ISS or the Russian space station *Mir* (Cucinotta et al., 2001).

Table 4-11(a). ***From Cucinotta et al. (2008): Comparison of Measured Organ Dose-equivalent for the STS-91 Mission by Yasuda et al. (2000) Using the Combined CR-39/TLD Method to HZETRN/QMSFRG Space Transport Model***

Tissue	Organ Dose-equivalent, mSv		
	Measured	HZETRN/QMSFRG	Difference (%)
Skin	4.5 ± 0.05	4.7	4.4
Thyroid	4.0 ± 0.21	4.0	0
Bone surface	5.2 ± 0.22	4.0	–23.1
Esophagus	3.4 ± 0.49	3.7	8.8
Lung	4.4 ± 0.76	3.8	–13.6
Stomach	4.3 ± 0.94	3.6	–16.3
Liver	4.0 ± 0.51	3.7	–7.5
Bone marrow	3.4 ± 0.40	3.9	14.7
Colon	3.6 ± 0.42	3.9	8.3
Bladder	3.6 ± 0.24	3.5	–2.8
Gonad	4.7 ± 0.71	3.9	–17.0
Chest	4.5 ± 0.11	4.5	0
Remainder	4.0 ± 0.57	4.0	0
Effective dose	4.1 ± 0.22	3.9	–4.9

Table 4-11(b). ***From Cucinotta et al. (2008): Comparison of Small Active Dosimetry Data from the ISS Expedition-2 Phantom Torso (July–August 2001) for Absolute Predictions for the HZETRN/QMSFRG Model. [Details on the measurement procedures are given in Badhwar et al. (2000)]***

Organ	Dose from Trapped Radiation, mGy/d		Dose from GCR, mGy/d		Total Dose, mGy/d		Difference (%)
	Expt.	Model	Expt.	Model	Expt.	Model	
Brain	0.051	0.066	0.076	0.077	0.127	0.143	13.3
Thyroid	0.062	0.072	0.074	0.077	0.136	0.148	9.4
Heart	0.054	0.061	0.075	0.076	0.129	0.137	6.7
Stomach	0.050	0.057	0.076	0.077	0.126	0.133	5.5
Colon	0.055	0.056	0.073	0.076	0.128	0.131	2.5

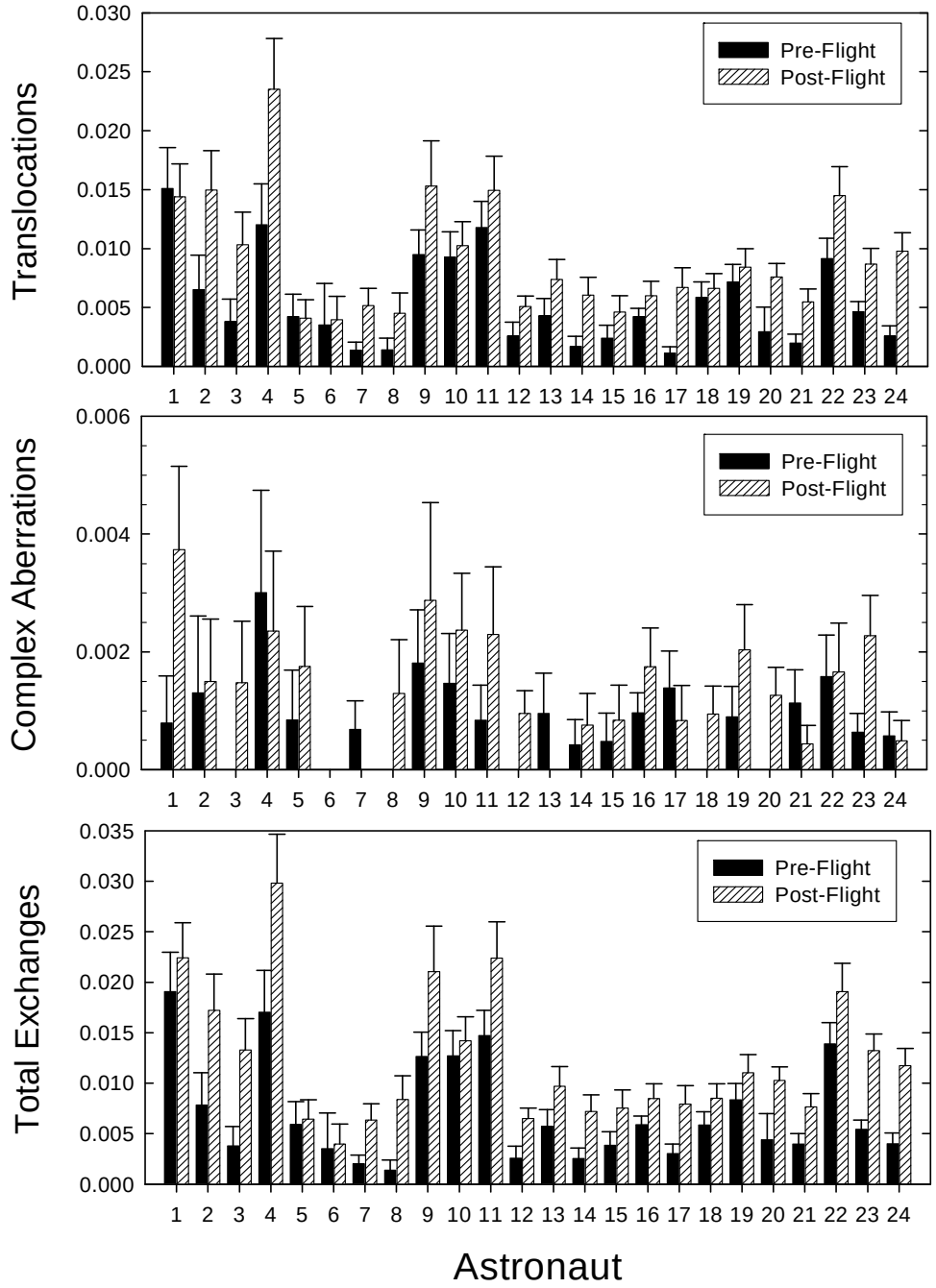

Figure 4-6. ***From Cucinotta et al. (2008): The frequency of translocations, complex aberrations, or total chromosome exchanges that is measured in each astronaut's blood lymphocytes before and after their respective space missions on ISS,*** **Mir,** ***or the space shuttle. An increase in total exchanges was observed for all astronauts. Translocations (22 of 24) and complex aberrations (17 of 24) increased in the majority of astronauts.***

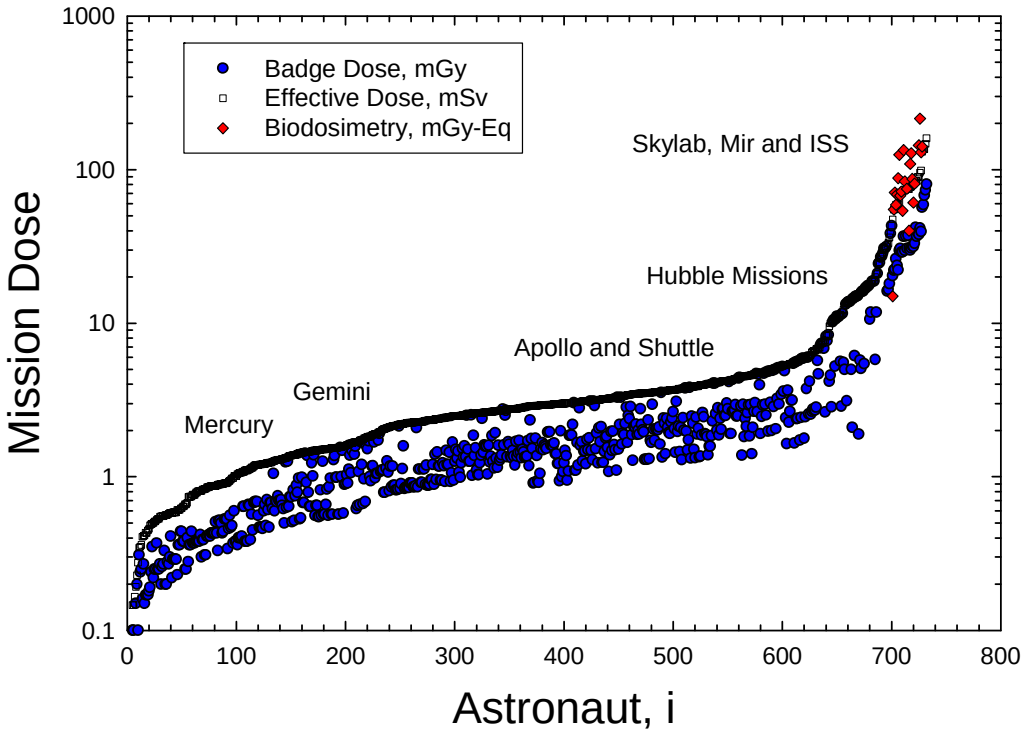

Figure 4-7. ***Summary of mission personnel dosimetry from all past NASA crews (Cucinotta et al., 2008). Effective dose and population average biological dose-equivalent for astronauts on all NASA space missions, including Mercury, Gemini, Apollo, Skylab, Apollo-Soyuz, space shuttle, shuttle-Mir, and ISS missions.***

Radiobiology evidence for protons and HZE nuclei

Studies with protons and HZE nuclei of RBEs for molecular, cellular, and tissue endpoints, including tumor induction, document the higher risk for space radiation components (NAS, 1996; NCRP, 2006; Cucinotta and Durante, 2006). This evidence must be extrapolated to the chronic conditions that are found in space and from the mono-energetic beams that are used at the NSRL and other accelerators to the complex mixed radiation types that are in space. Sufficient proof that experimental models represent cancer processes in humans, including estimating the effectiveness of shielding and biological countermeasures, must be obtained for high-risk missions where acceptable levels of cancer risks are approached or, perhaps, exceeded. Evidence and progress in these areas is described next.

Cancer Induction by Space Radiation

A necessary step for improving space radiation cancer risk assessment is to perform studies on the molecular pathways that are causative of cancer initiation and progression, and to extend these studies to learn how such pathways can be disrupted by HZE ions, including both genetic and epigenetic modifications that are noted as the hallmarks of cancer (figure 4-8). The goal of this research is to establish a more mechanistic approach to estimating risk and to answer questions, including whether HZE effects can be scaled from those of gamma rays, whether risk is linear with low dose-rate, and how individual radiation sensitivity impacts the risks for astronauts, a population that is selected for many factors related to excellence in health.

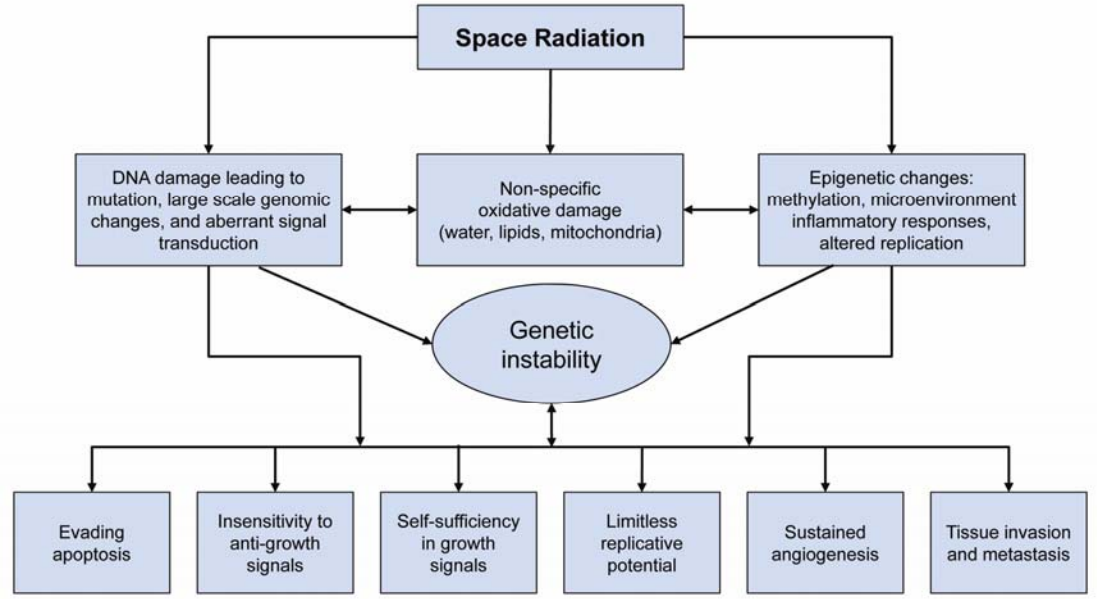

Figure 4-8. ***The hallmarks of cancer (Hanahan and Weinberg, 2000) and possible mechanisms of radiation damage that lead to these changes observed in all human tumors.***

The Initial Biological Events

Energy deposition by HZE ions is highly heterogeneous with a localized contribution along the trajectory of each particle and lateral diffusion of energetic electrons (delta rays) that are many microns from the ions path (Goodhead, 1994; Cucinotta et al., 2000b). These particles are, therefore, characterized by a high LET; however, they contain a low-LET component due to the high-energy electrons that are ejected by ions as they traverse tissue. Biophysical models have shown that the energy deposition events by high-LET radiation produce differential DNA lesions, including complex DNA breaks, and that there are qualitative differences between high- and low-LET radiation, in both the induction and the repair of DNA damage (Prise et al., 1998; Sutherland et al., 2000; Rydberg et al., 2005). The number of DNA single-strand breaks (SSBs) and DSBs that are produced by radiation varies little with radiation type; however, for high-LET radiation, a higher fraction of DNA damages are complex; i.e., clusters containing mixtures of two or more of the various types of damages (SSB, DSB, etc.) within a localized region of DNA. Complex damage is uncommon for endogenous damage or low-LET radiation, and has been associated with the increased RBE of densely ionizing radiation. The repair of DSB is known to occur through direct end-joining and homologous recombination processes. Indications are that (1) for high-LET radiation, where complex DSBs occur with high frequency, little repair occurs, leading to cell death; or (2) the mis-rejoining of unrepairable ends with other radiation-induced DSB leads to large DNA deletions and chromosome aberrations. While the high effectiveness in cell killing provides the rationale for heavy-ion cancer therapy (hadrontherapy), residual damage in surviving cells is of concern for carcinogenesis.

Chromosome damage and mutation

Heavy charged particles are very effective at producing chromosomal exchanges with RBE values exceeding 30 in interphase (as visualized using premature chromosome condensation) and 10 at the first post-irradiation mitosis for energetic Fe-ions (George et al., 2003). The detailed RBE vs. LET relationship that was found for total exchanges is similar to that of earlier studies of mutation (Kiefer et al., 1994; Kiefer, 2002) and in

vitro neoplastic transformation (Yang et al., 1985). For all of these endpoints, RBE peaks at around 100 to 200 keV/µm before it decreases at very high-LET. However, the quality of chromosome damage is different when heavy ions are compared to sparsely ionizing radiation. Large differences in gene expression are observed between X rays and HZE ions, thus reflecting differences in damage response pathways (Ding et al., 2005; Chang et al., 2005). Qualitative differences in the type of gene mutations have also been reported (Kronenberg, 1994; Kronenberg et al., 1995). Novel multicolor fluorescence painting techniques of human chromosomes have clearly demonstrated that high-LET α-particles and Fe-ions induce many more complex types of chromosomal exchanges in human cells than low-LET radiation. Most of these complex chromosomal rearrangements will ultimately lead to cell death. In fact, only a small fraction of the initial damage is transmitted in mice 2 to 4 months after the mice have been exposed to energetic Fe-ions. A low RBE for the induction of late chromosomal damage has also been measured in the progeny of human lymphocytes that were exposed in vitro to energetic Fe-ions, with the interesting exception of terminal deletions, which occurred with much higher frequency in the progeny of cells that were exposed to heavy ions compared to gamma rays (Durante et al., 2002).

Genomic instability

Genomic instability has been observed both in vitro and in vivo in the progeny of cells that are irradiated with heavy ions in several model systems (NCRP, 1997a). The presence of chromosomes that are lacking telomeres in the progeny of cells that were exposed to heavy ions is particularly interesting. Sabatier et al. (1992; 2005) found that rearrangements involving telomere regions are associated with chromosomal instability in human fibroblasts that occur many generations after exposure to accelerated heavy ions. Telomere dysfunction plays a crucial role in initiating or sustaining genomic instability, which is a major step in cancer progression. Heavy-ion-induced effects on telomere stability have also been studied using siRNA (small interfering ribonucleic acid) knockdown for components of DNA-dependent protein kinase (DNA-PK) in human lymphoblasts. Differential results were found for gamma rays and HZE nuclei, with iron nuclei being much more effective in producing DSB-telomere fusions after knockdown of DNA-PK (Zhang et al., 2005). Cells containing telomere-deficient chromosomes will either senesce or undergo breakage-fusion-bridge (B/F/B) cycles, thereby promoting genetic instability. The fate of normal cells that contain a single terminal deletion is unknown, but it has been shown that the loss of a single telomere in cancer cells can result in instability in multiple chromosomes (Feldser et al., 2003; Maser and DePinho, 2002). These recent results suggest that telomere instability could be an important early event in the pathway to cancer induction by HZE nuclei.

Cancer and tissue effects

Animal studies generally demonstrate that HZE nuclei have higher carcinogenic effectiveness than low-LET radiation. The number of studies of animal carcinogenesis with HZE nuclei is extremely limited, as summarized in Table 4-12. Relative biological effectiveness factors comparing gamma rays to HZE ions were measured in mice or rats for tumors of the skin (Burns et al., 1993) and of the Harderian (Fry et al., 1985; Alpen et al., 1993) or mammary gland (Dicello et al., 2004), reaching values as high as 25 to 50 at low doses. However, the risk and detriment of cancer will not be fully characterized until the relationship between radiation quality and latency, where tumors appear earlier after high-LET irradiation, is adequately described. The earlier latency and increasing effectiveness that is found with HZE ions that are similar to those in earlier studies with neutrons (Ullrich, 1984; Fry and Storer, 1987), together with the lack of response of gamma rays that is seen in many low-dose studies, suggests that the scaling concepts that are used in current risk assessment approaches are unable to describe important qualitative effects, and that relative biological effectiveness factors may, in principle, be indefinable or a faulty concept.

Table 4-12. ***Tumor Induction Studies with HZE Nuclei***

Tumor Model	End-point	HZE type	Reference
Mice (B6CF1)	Life-shortening	C, Ar, Fe	Ainsworth (1986)
Mice (B6CF1)	Harderian gland	He, C, Ar, Fe	Fry et al. (1985)
Mice (B6CF1)	Harderian gland	He, Ne, Fe, Nb	Alpen et al. (1993)
Rat (Sprague-Dawley)	Skin tumors	Ne, Ar, Fe	Burns (1992)
Rat (Sprague-Dawley)	Mammary tumors	Fe	Dicello et al. (2004)
Mice (carcinoma-bearing animal (CBA))	Leukemia, liver tumors	Fe, p, Si	Ullrich, in preparation

Recent studies have debated the relative importance of DNA damage and mutation or extracellular matrix remodeling and other non-targeted effects as initiators of carcinogenesis (Barcellos-Hoff et al., 2005). Tissue effects that are independent of DNA damage and that have been associated with cancer initiation or progression include genomic instability (Park et al., 2003), extracellular matrix remodeling, persistent inflammation, and oxidative damage (Mothersill and Seymour, 2004). Other studies are exploring possible relationships between radiation and the activation of dormant tumors and the modulation of angiogenesis (Folkman et al., 1989).

So-called bystander or non-targeted effects may have enormous consequences for space exploration. Non-targeted effects may lead to a supra-linear dose-response curve at low doses, perhaps reducing the effectiveness of spacecraft shielding; but it may also provide protection by removing damaged cells from the organism. Both effects challenge the conventional linear no-threshold risk model assumption, which is currently adopted for radioprotection on Earth and in space. These effects also suggest important targets for biological countermeasures that are likely to be more effective than are countermeasures that target DNA damage.

Results in tissues suggest that differences in biological response between high and low LET differ depending on the model context that is considered (i.e., 2D vs. 3D vs. animal). As a result of the many types of particles, energies, and doses of interest that are in space, extensive animal experimentation has been prohibited by costs in the past. More recently, however, studies in 3D human coculture are proving to be an effective method with which to study cancer risks in a more realistic context (Barcellos-Hoff et al., 2005; Riballo et al., 2004).

Models of Cancer Risks and Uncertainties

Life-table methodology

The double-detriment life-table is the approach that is recommended by the NCRP (NCRP, 2000) to estimate radiation cancer mortality risks. In this approach, the age-specific mortality of a population is followed over its entire life span with competing risks from radiation and all other causes of death described (Bunger et al., 1981). For a homogeneous population receiving an effective dose E at age aE, the probability of dying in the age-interval from a to $a+1$ is described by the background mortality-rate for all causes of death, $M(a)$, and the radiation cancer mortality rate, $m(E,a_E,a)$, as

$$q(E,a_E,a) = \frac{M(a)+m(E,a_E,a)}{1+\frac{1}{2}[M(a)+m(E,a_E,a)]} \quad (7)$$

The survival probability to live to age, *a,* following an exposure, E, at age, a_E, is

$$S(E, a_E, a) = \prod_{u=a_E}^{a-1} [1 - q(E, a_E, u)] \quad (8)$$

The excess lifetime risk (ELR), which is the increased probability that an exposed individual will die from cancer, is defined by the difference in the conditional survival probabilities for the exposed and the unexposed groups as

$$ELR = \sum_{a=a_E}^{\infty} [M(a) + m(E, a_E, a)] S(E, a_E, a) - \sum_{a=a_E}^{\infty} M(a) S(0, a_E, a) \quad (9)$$

A minimum latency-time of 10 years is often used for low-LET radiation (NCRP, 2000); however, alternative assumptions should be considered for high-LET radiation. The REID, which is the lifetime risk that an individual in the population will die from a cancer that is caused by his or her radiation exposure, is defined by

$$REID = \sum_{a=a_E}^{\infty} m(E, a_E, a) S(E, a_E, a) \quad (10)$$

In general, the value of the REID exceeds that of the ELR by about 10% to 20%. Vaeth and Pierce (1990) have discussed cases in which the ELR is ill-defined and suggested that the REID is the preferred quantity for radiation protection. The loss of life-expectancy among exposure-induced-deaths (LLE-REID) is defined by (Vaeth and Pierce, 1990)

$$LLE - REID = \frac{LLE}{REID} \quad (11)$$

where the average loss of life-expectancy, *LLE*, in the population is defined by

$$LLE = \sum_{a=a_E}^{\infty} S(0, a_E, a) - \sum_{a=a_E}^{\infty} S(E, a_E, a) \quad (12)$$

Radiation Carcinogenesis Mortality Rate

For projecting lifetime cancer fatality risks, an age- and gender-dependent mortality rate per unit dose, which is estimated for acute gamma-ray exposures, is multiplied by the radiation quality factor and reduced by the DDREF (NCRP, 2000). The additivity of effects of each component in a radiation field is assumed. Radiation mortality rates are largely modeled using the Japanese atomic-bomb survivor data. For transferring risks from the Japanese to the U.S. population, two models are often considered. A multiplicative transfer model assumes that radiation risks are proportional to spontaneous or background cancer risks. The additive transfer model assumes that radiation risk acts independently of other cancer risks. However, the NCRP (NCRP, 2000) recommends that a mixture model be used that contains fractional contributions from the multiplicative risk model or additive risk model. The radiation mortality rate is

$$m(E, a_E, a) = [\nu ERR(a_E, a) M_c(a) + (1-\nu) EAR(a_E, a)] \frac{\sum_L Q(L) F(L) L}{DDREF} \quad (13)$$

where the *ERR* and *EAR* are the excess relative risk and excess additive risk per Sievert, respectively, $M_c(a)$ is the gender- and age-specific cancer mortality rate in the U.S. population, *F* is the tissue-weighted fluence, and *L* is the LET. In Eq(13), ν is the fractional division between the assumption of the multiplicative and additive risk transfer models. For solid-cancer, it is assumed that ν=1/2; for leukemia, it is assumed that ν=0.

Uncertainties in the Projection Model

Equation (13) consists of a product of several factors: the *ERR* or *EAR*, the background cancer rates, M_c, the effective dose represented by the physical dose, *F(L)*, times the radiation quality factor, *Q(L)*, and the dose and dose-rate reduction factor, *DDREF*. The limiting behavior of the addition of many random variables is well known as the normal distribution. In contrast, the limiting behavior of the multiplication of many random factors will be a log-normal distribution. Equation (7) assumes that each multiplicative factor is independent. This assumption may not be strictly valid, however, because of the possible correlations between factors or non-additivity of different radiation components, since the cells will be traversed by multiple particles and delta rays that are produced by ions passing through adjacent cell layers (Cucinotta et al., 1998b). As the risk for longer-duration missions exceeds a few percent, the upper 95% C.I.s may exceed 10%. In such cases, the Monte-Carlo sampling of mortality rates to estimate uncertainty bands is insufficient, and the expression for the REID that is given by Eq(10) must be used because of competing risks from other causes of death that will reduce the likelihood of very large radiation risks. Therefore, in the sampling approaches that are described below, trials are accumulated for the REID rather than the mortality rate. A criteria that is used to formulate probability distribution functions (PDFs) for various factors is to ensure that the PDFs are peaked at the values that are recommended by the NCRP (NCRP, 2000), such as the DDREF and Q, or in the current physics models of radiation environments and transport that are used in mission projections or spacecraft designs. We next discuss the uncertainties in the projection model.

Uncertainties in Low-LET Epidemiology Data

For Monte-Carlo sampling purposes, the low-LET mortality-rate per Sievert, m_l, is written

$$m_l(E, a_x, a) = \frac{m_0(E, a_x, a)}{DDREF} \frac{x_D x_s x_T x_B}{x_{Dr}} \quad (14)$$

where m_0 is the baseline mortality rate per Sievert (see Eq(13)) and the x_α are quantiles (random variables) whose values are sampled from associated PDFs, $P(x_\alpha)$. Note that the DDREF applies only to the solid cancer risk and not to the leukemia risk under the stated assumptions. The NCRP Report No. 126 (NCRP, 1997a) defines the following subjective PDFs, $P(x_\alpha)$, for each factor that contributes to the acute low-LET risk projection:

1. $P_{dosimetry}$ represents the random and systematic errors in the estimation of the doses received by atomic-bomb blast survivors. It is assumed as a normally distributed PDF for bias correction of random and systematic errors in the dosimetry (DS86) with mean 0.84 and standard deviation 0.11.

2. $P_{statistical}$ represents the distribution in uncertainty in the point estimate of the risk coefficient, r_0. It is assumed as a normally distributed PDF with a mean of 1 and a standard deviation of 0.15.

3. P_{bias} represents any bias resulting for over- or under-reporting cancer deaths. P_{bias} is assumed as a normal distribution with a most probable value of 1.1 and a 90% C.I. from 1.02 to 1.18 corresponding to a standard deviation of 0.05.

4. $P_{transfer}$ represents the uncertainty in the transfer of cancer risk following radiation exposure from the Japanese population to the U.S. population. Both additive and relative risk models were considered by NCRP Report No. 126 (NCPR, 1997a) in assessing the uncertainties in such transfer. $P_{transfer}$ is log-normal with a mean of 1 and a standard deviation of 0.26 (geometric standard deviation (GSD)=1.3).

5. P_{Dr} represents the uncertainty in the knowledge of the extrapolation of risks to low dose and dose-rates, which are embodied in the DDREF. The NCRP assumes P_{Dr} to be a truncated triangle distribution starting at 1 and ending at 5 with a peak at 2 and a relative value of 1/4 or 1/2 at 1 or 5, respectively, compared to the peak values for the DDREF at 2. This PDF is used to scale the low-LET risk coefficient (mortality rates) in our estimates for space radiation.

The NCRP also considered a PDF for bias correction to project cancer risks over a lifetime. It is ignored herein because the astronaut population is generally over age 30 years and the Japanese data are now complete for these ages. We also ignore the assumed "unknown uncertainties" from NCRP Report No. 126 (NCRP, 1997a).

Uncertainties due to Dose-Rate and Protraction Effects for Ions

For a low dose-rate and protracted proton and HZE radiation exposure of more than a few months, new biological factors may influence risk assessments, including redistribution in the cell cycle, repopulation, or promotional effects, especially when particle fluences are sufficiently large to lead to multiple hits of target cells or surrounding cells and tissue environments. Not only are there no human data for protons and HZE ions, there are also very little experimental data at low dose-rates for these particles. Confidence in using radio-epidemiological data for acute (atomic-bomb survivors) or fractionated (patient) data is decreased when it is applied to protracted exposure. Experimental data for protracted proton or heavy ion irradiation in experimental models of carcinogenesis are almost nonexistent. Burns et al. (1994) found that split doses of argon ions that were separated by a few hours up to 1 day increased the risk of skin cancer in rats. Alpen et al. (1994) found that for Harderian gland tumors in mice, using seven 2-week fractions of 0.07 Gy of iron increased risk by 50% as compared to a single acute dose of 0.4 Gy. A study of chromosomal aberrations in human lymphocytes (George et al., 2001), for both acute and low dose-rates (0.08 Gy/hr) with 250 MeV protons, showed less sparring than was found for gamma rays. The Skyhook study (Ainsworth et al. (1986)) considered life-shortening in mice by comparing single acute with weekly fractions of several ions, but the results were unclear with regards to any increase or decrease in risk.

A good number of studies for cancer induction or life-shortening in mice exist for gamma rays and neutrons; these studies show both sparring effects for gamma rays and that neutron effects may be increased due to protraction under certain conditions in some tissues (Ullrich, 1984; NCRP, 1990). Important questions related to the differences in life span, cell turnover rates, or the mechanisms of initiation or promotion in humans and mice make estimates of the effects of protraction on risk difficult. If protraction effects do increase the risk from high-LET radiation, such effects would be more important for a Mars mission than for the shorter lunar missions. In space, each cell will be traversed about every 2 to 3 days by a proton or delta ray that is produced by ions in adjacent cells, and with a decreasing frequency of from weeks to months as the charge of the HZE nuclei increases (Cucinotta et al., 1998b). Studies of mixed-fields of protons and HZE ions are needed to understand the uncertainties in dose-rate and protraction effects from space radiation. Uncertainties that

are related to radiation quality, dose-rate, and protraction could lead to correlations that will be difficult to describe when based on limited experimental data. Methods to treat correlation effects will be needed when the data on protraction effects become available.

Radiation Quality and Latency or Temporal Patterns of Risk

An additional radiation quality uncertainty is introduced by the scaling assumption that is used in Eq(13) because the time dependence for low- and high-LET radiation is assumed to be identical. Data on tumors or genomic instability in mice with neutrons (Ullrich, 1984; Ulrich and Ponnaiya; NCRP, 1990) and the studies of rat or mammary carcinogenesis with HZE nuclei (Burns et al., 1994; Dicello et al., 2004) suggest that the latency time is appreciably reduced for high-LET radiation compared to low-LET radiation. Sparse data are available to estimate the impact of these differences on uncertainties. A radiation quality-dependent latency is more important in the additive transfer model than in the multiplicative transfer model, especially at younger ages of exposure. We ignore these uncertainties, however, and replace the 10-year minima latency assumption that is made for low LET with the step-in latency model (Pierce et al., 1996) that is used for the leukemia risk. The effects of these assumptions will need to be addressed when data and knowledge on underlying mechanisms become available.

Uncertainties in Quality Factors

Radiation quality factors represent the largest uncertainty when estimating space radiation cancer risks. Past reviews on the relative biological effectiveness of high-LET radiation include International Commission on Radiation Units (ICRU) Report No. 40 (1986), NCRP Report No. 104 (1990), and, more recently, ICRP Report No. 92 (2003). The practice of assigning radiation quality factors that are followed by committees considers an average of the RBE factors at low doses (RBE_{max}) for the most relevant experimental endpoints. Uncertainties in the assignment of RBEs for protons and heavy ions arise for several reasons, including sparseness of data for tumorigenesis in animal models, surrogate tissue, or cellular endpoints; variability in reference radiation and doses and dose-rates employed; and lack of data over the LET range of interest. Linearity at low dose or dose-rates for the reference radiation or ions also is often not sufficiently established in experiments. Statistical limitations frequently hinder studies at the low dose-rates of interest for space radiation protection. For high-LET radiation, a turnover or bending that is found in the dose response for tumor induction and neoplastic transformation is observed at moderate doses, thus presenting further uncertainties in estimating the effectiveness of high-LET radiation at low dose-rates.

Figure 4-9 provides representative examples of the ratio of RBE_{max} to Q for mouse tumors, cell transformation or mutations, or cytogenetic endpoints. The ratio is often two to three times higher or lower than unity, which indicates the expected deviation from Q in available data.

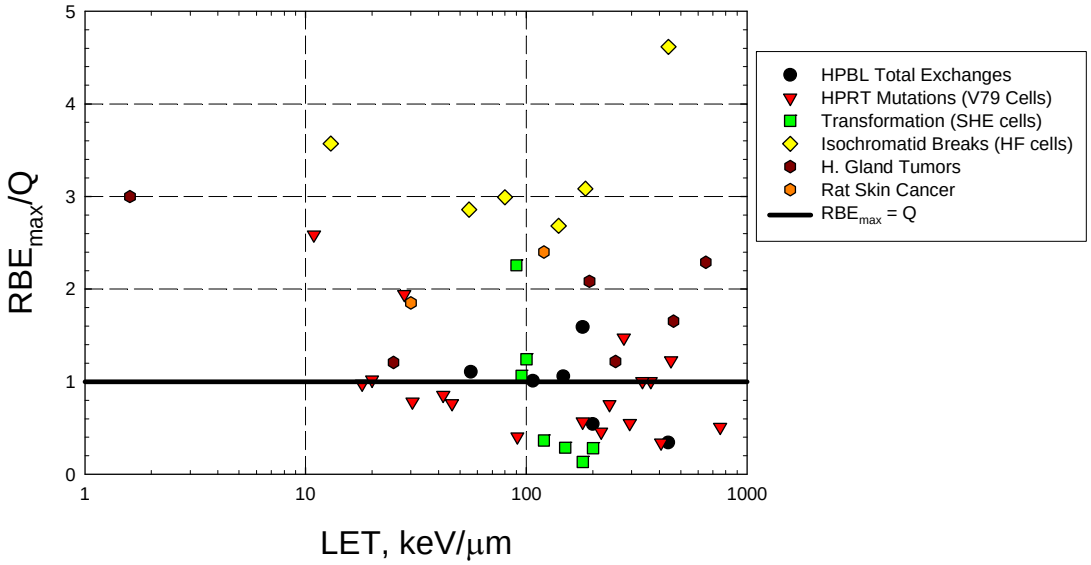

HPBL – human peripheral blood leukocyte; HPRT – hypoxanthine-guanine phosphoribosyltransferase; SHE – Syrian hamster embryo; HF – human fibroblast

Figure 4-9. ***Comparison of ratio of* RBE$_{max}$ *to* Q *for several endpoints found with proton, α-particle, and heavy ion irradiations (reference experiments listed in Table 4-1).***

Table 4-13 shows the LET values at the maximum RBE that was found in past studies that were selected from experiments in which more than five ions were employed. Large deviations from the Q peak at 100 keV/µm are observed in these experiments, with a range from about 50 to 190 keV/µm for the peak. These data are largely derived from the facilities at Berkeley, Calif., Darmstadt, Germany, Chiba, Japan, and the Alternating Gradient Synchrotron (AGS), Brookhaven National Laboratory, Upton, N.Y. The number of past studies and endpoints that were used are limited if they are viewed as surrogate endpoints for human carcinogenesis. Additional data for more appropriate endpoints should become available in the next few years from the NSRL. Track structure models suggest that each ion species would have distinct RBE curves that are of similar shape, with curves for lower-charge ions peaking at a lower LET than for higher-charged ions (Katz et al., 1971; Cucinotta et al., 1996; Nikjoo et al., 1999). Furthermore, above about 1 MeV/u, lower-charged ions have a higher biological effectiveness than higher-charged ions of identical LET. Based on track structure models, we expect that the data sets that consider only a few ions are insufficient for defining the radiation quality dependence of *Q*. LET response curves also are predicted to depend on the target size (e.g., for gene or chromosome region) and intrinsic radiation sensitivity, which includes competition with cell death. These factors likely vary between tissues.

Table 4-13. ***Approximate LET in which Maximum RBE Was Found in Biological Experiments***

Biological System	Endpoint	LET at Peak RBE, keV/µm	LET range (no. of ions studied)	Reference
Human TK6 lymphoblasts cells	TK (triose-kinase) mutants	60	32–190 (6)	Kronenberg (1994)
Human TK6 lymphoblasts cells	HPRT mutants	60	32–190 (6)	Kronenberg (1994)
Human lung fibroblasts	HPRT mutants	90	20–470 (9)	Cox and Masson (1979)
Human skin fibroblasts	HPRT mutants	150	25–920 (7)	Tsuoboi et al. (1992)
V79 Chinese hamster cells	HPRT mutants	90	10–2,000 (16)	Kiefer et al. (1994); Belli et al. (1993)
Caenorhabditis elegans	Recessive lethal mutations	190	0.55–1,110 (14)	Nelson et al. (1989)
Human lymphocyte cells	Chromosomal exchanges	147	0.4–1,000 (10)	George et al. (2003)
Human fibroblast cells	Chromatid breaks	80–185	13-440 (6)	Kawata et al. (2001)
C3H10T1/2 mouse cells	Transformation	140	10–2,000 (10)	Yang et al. (1989)
C3H10T1/2 mouse cells	Transformation	90	20–200 (10)	Miller et al. (1995)
SHE cells	Transformation	90	20–200 (8)	Martin et al. (1995)
Mouse ($B6CF_1$)	H. gland tumors	185*	2–650 (6)	Fry et al. (1985)
Mouse ($B6CF_1$)	H. gland tumors	193	0.4–1,000 (7)	Alpen et al. (1993)
Mouse ($CB6F_1$)	Days life lost	52*	50–500 (6)	Ainsworth (1986)

*Track-segment or spread-out Bragg peak (SOBP) irradiations.

To account for the uncertainties in quality factors, Cucinotta et al (2006) recommend a trial function that has a shape that is guided by both experimental data and biophysical models, and a sample from distributions of parameters that enter into the functional form. The *Q(L)* trial function is defined as

$$Q_{trial}(L) = \begin{cases} 1 & L < L_0 \\ AL - B & L_0 \le L < L_m \\ C / L^p & L \ge L_m \end{cases} \quad (15)$$

The values of L_0, L_m, and p, and the maximum value, $Q_m(L_m)$, which are derived from the PDFs, are described below. Using Eq(15), one can solve for the values of the constants A, B, and C. Often-discussed issues on the definition of *Q(L)*, as embodied in Eq(15), are the value of the slope *p* that controls the decrease in *Q(L)* above a maximum, the maximum value of *Q(L)*, the LET where the maximum occurs, L_m, and the minimum LET where *Q(L)* rises above unity, L_0. We note that the ICRP-60 (ICRP 1991) Q-function corresponds to L_0=10 keV/µm, L_m=100 keV/µm, p = 0.5, and Q_m=30 such that A=0.32, B=2.2, C=300, and the ICRP-26 Q-function, L_0=3.5 keV/µm, L_m=172.5 keV/µm, p = 0, and Q_m = 20.

The parameter samplings are based on the following assumptions for PDFs:

a. L_0: equal probability between 5 and 10 keV/µm, and decreasing to zero at 1 keV/µm, or above 15 keV/µm.
b. L_m: equal probability for LET values between 75 and 150 keV/µm, and decreases to zero at 50 keV/µm or above 250 keV/µ m.
c. p: equal probability between p = 1/2 and 1, and decreasing to zero at p<0 or p>2.
d. Q_m: log-normal distribution with a mean value of 30 and a geometric standard deviation (GSD) of 1.8.

Figure 4-10 shows examples of trial *Q(L)* functions that contribute in the sampling procedures, and figure 4-11 shows the resulting average *Q(L)* and 95% C.I. after 20,000 trials. The resulting range is smaller than in the previous Cucinotta et al. report (2001b); however, it should be a reasonable estimate when the effects of dose protraction are not included in the uncertainty analysis.

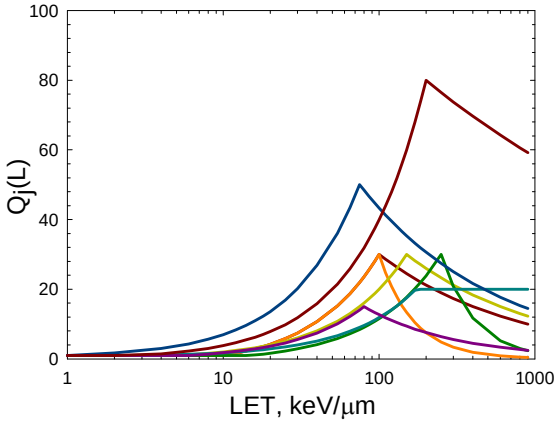

Figure 4-10. ***Examples of trial quality factor functions used in uncertainty calculations. A distinct curve is generated for each trial.***

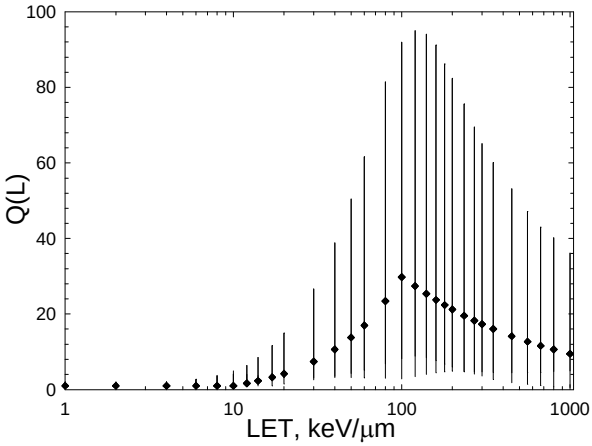

Figure 4-11. ***Average quality factor (circles) and 95% C.I.'s vs. LET that is derived from Monte-Carlo sampling over trial function of Eq(15).***

Uncertainties in Physics: Environments and Transport Codes

Space dosimetry and radiation transport codes have been studied extensively in the past, and although no major scientific questions led to errors in the assessment of space radiation environments, there are uncertainties due to the limitations in the dosimetry that was flown on past space missions. For application of computational models, the level of detail that has been used in transport code comparisons is often limited,

with common simplifications including the use of an aluminum-equivalent shielding approximation, simplified geometries, and no description of orientation effects. Approaches to assess errors in space dosimetry include the inter-comparison of different dosimetry on the same missions and to the results of space radiation transport models. Although statistical errors in the assessment of physical doses are quite small (<5%), the inter-comparisons between laboratories have shown differences on the order of 10% for absorbed dose (Badhwar, 1997). Comparisons of transport calculations to measurements of LET spectra or dose equivalencies should consider the response functions of different detector types to charged particles or neutrons (Nikjoo et al., 2002). Commonly used detectors are TEPCs, silicon detectors, and CR-39 plastic track detectors. Good agreement has been found in the limited number of comparisons that have been made (e.g., Badhwar and Cucinotta, 2000; Kim et al., 2003; Shinn et al., 1998), especially when detector response functions are represented in the comparisons.

Models of the GCR environment rely on the large number of space flight and balloon measurements that have been made, and apply the diffusion theory of Parker (1965) to describe the modulation of the GCR over the solar cycle. The root mean square error for GCR environmental models is less than 7% for the major GCR elements and less than 12% for most minor elements (Badhwar and O'Neill, 1994a; Badhwar et al., 1994b; O'Neill, 2005). Data from the advance composition explorer (ACE) are further improving these models (figure 4-12).

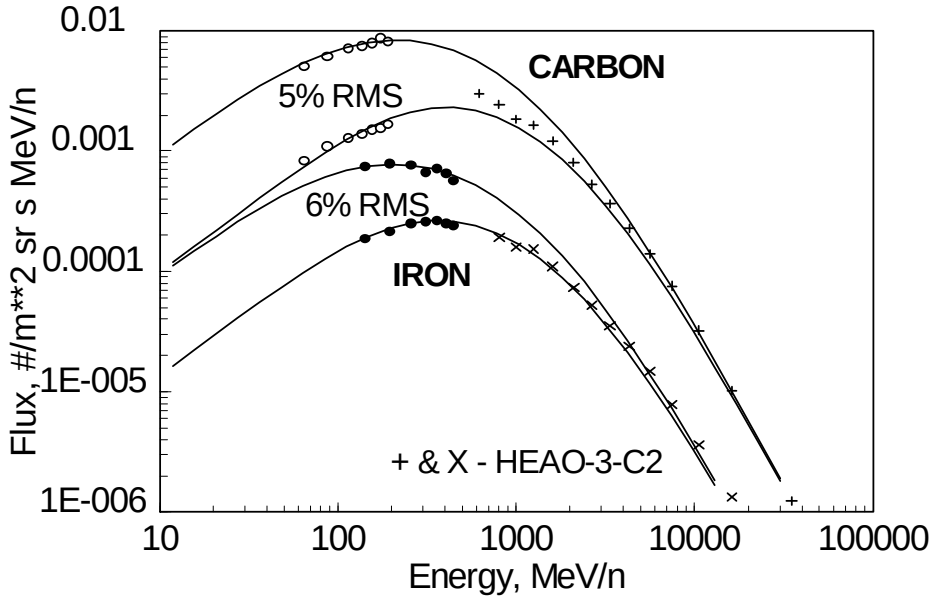

Figure 4-12. ***From O'Neill (2005) Differential flux energy spectra near solar minimum and maximum for two of the more-abundant elements, typical of the better fits. The symbols represent the measured values that are described in O'Neill (2005) and lines in the Badhwar-O'Neill GCR model.***

The isotopic composition of the GCR is also represented in the transport codes (Cucinotta et al., 2003b) that are used in risk calculations. Solar particle event spectra vary from event to event, and there is no method that is available to predict the fluence, energy spectra, or dose-rates of a future event. In this chapter, we discuss calculations for the large SPE of August 1972. Transport codes rely on databases for nuclear interaction cross sections, including inclusive single differential in energy or total fragment production cross sections for projectile

fragments, as well as double differential in energy and angle for lighter mass secondaries (i.e., neutrons, H-ions and He-ions, and mesons). Cross-section data are sparse for some projection-target combinations and in the number of energies, especially above 1,000 MeV/u. Three-dimensional aspects of transport from angular scattering, which is a small correction for high-energy ions, are expected to be an important correction for neutrons and other light mass ions. Computer codes that use multigroup methods or Monte-Carlo simulations to describe angular effects on neutron transport have been developed for GCR shielding applications. The Monte-Carlo codes are limited by the computational times that are needed to describe spacecraft with thousands of parts, and the multigroup methods are limited by the ability to describe complex geometries. However, because flight measurements and the results of the HZETRN code (Wilson et al., 1995) using the Badhwar-O'Neill GCR input spectra (Badhwar and O'Neill, 1994) and QMSFRG (quantum multiple scattering fragmentation) nuclear interaction data base (Cucinotta et al., 2003a) are in good agreement, it is unclear whether such developments will have an important impact on risk assessment.

Differences between transport models and flight dosimetry that account for the response of the detector to different radiation components are generally small, with absolute differences within 10% for the GCR dose and 20% for the GCR dose-equivalent (Badhwar, 1997; Badhwar and Cucinotta, 2000 Cucinotta et al., 2000b; Cucinotta et al., 2003b). However, measurements of dose or dose-equivalent may not provide sufficient information on possible errors in predicting the LET spectra because compensating errors can occur. Neutron spectra also are difficult to assess within complicated spacecraft and tissue geometries. In particular, measurements or calculations of neutron spectra are expected to lead to uncertainties in LET spectra in the LET range from about 30 to 300 keV/μm where recoil nuclei deposit the majority of the energy. Neutrons also cause a low-LET gamma-ray component that is often ignored in calculations. Larger errors are expected at a higher LET, where stopping nuclei, which may be difficult to define due to local tissue variations, dominate. We expect uncertainties to be larger at high-LET values, where the role of local target recoils and stopping GCR primaries are difficult to describe.

The PDFs for the uncertainties in LET spectra should ensure that the resulting dose-equivalent is consistent with the transport code comparisons to past space flight measurements for GCR. A quantile, x_L, which is associated with a normal distribution, $P_F(x_F=F/F_0)$ – where x_F is the ratio of sampled estimate of the fluence, F, to the point estimate, F_0, from the HZETRN code – is used with a standard error that increases with LET to represent the higher uncertainties that are expected for prediction of neutron effects and the difficulty in precisely defining stopping ions in complex geometries. The PDF is given a median of x0F=0.65 to ensure that the resulting dose-equivalent is in agreement with values from prior comparisons between the transport codes and flight measurements that were cited above. Standard deviations for different LET regions are given in Table 4-14 (right).

Table 4-14. ***Standard Deviations for Uncertainties in Model LET Spectra for Several LET Regions***

LET Interval	SD for dF/dL
< 30 keV/μm	1.0
30–300 keV/μm	2.0
> 300 keV/μm	2.5

Figures 4-13 and 4-14 illustrate the errors that are assigned to environmental and physical factors in evaluating LET spectra at tissue sites.

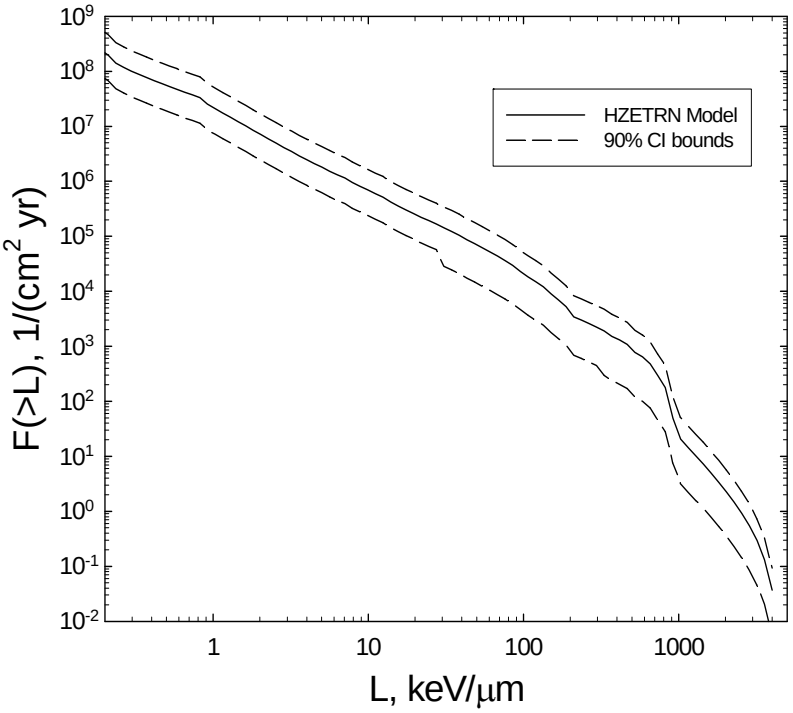

Figure 4-13. ***Calculation of tissue-weighted integral LET spectra and 90% C.I. for space environmental and transport uncertainties for a 20-g/cm^2 aluminum shield for 1 year in deep space.***

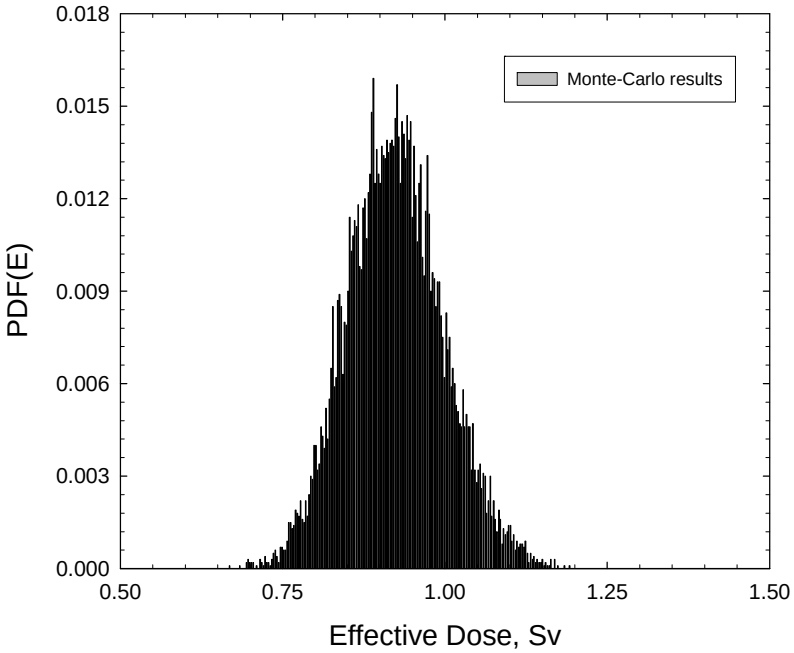

Figure 4-14. ***PDF for GCR effective dose for 20-g/cm^2 aluminum shield for 600-d Mars swing-by mission. The point estimate is 0.86 Sv, and the 95% C.I. for uncertainties in LET distribution at tissue sites is [0.78, 1.08] Sv. Only uncertainties in physics are included.***

Uncertainties due to Life-tables and Population Cancer Rates

Although radiation risk calculations are based on population data, they are used to estimate risks for individuals. Population data reflect gender differences, but also change with calendar year and often are used to make projections far into the future. For the astronaut population, the appropriateness of using the U.S. average population in making projections can be questioned because the so-called "healthy worker" effect is expected for astronauts. In the average U.S. population, females have longer life spans than males, partly due to their overall lower risk of cancer. The formalism of Eq(7) through Eq(13) shows two counteracting effects arising when one attempts to determine whether the use of population rates that are representative of a healthier population compared to the U.S. population would decrease or increase the risk of radiation carcinogenesis.

First the population survival function acts to decrease radiation risks, especially at older ages. An improved survival function that acts alone will, therefore, increase the risk from radiation. However, an improved survival function also suggests lower background cancer rates, which makes up some fraction of the delay in mortality. In the multiplicative transfer model, radiation risks are reduced if a healthy worker effect is due, in part, to a reduced natural incidence of cancer. Thus, the portions of the risk transfer that are assigned to multiplicative and additive transfer act in opposition if a healthy worker effect is present.

In a model where a geometric average of these two models is used, we expect a minor change if an improved life-table and background cancer rates are assumed. The role of the survival function is also reduced if solid cancers would display a plateau at long times after exposure (>30 years), as has been suggested in some studies (Preston et al., 2003). This discussion points to the need for better understanding of the biological basis for risk transfer models and dependence of risk after long follow-up times. Cucinotta et al. (2006) considered projections of life expectancy that were made by the Social Security Administration (SSA, 2006) and differences in rates between males and females to estimate errors in the life-table formalism. Uncertainties, which can be on the order of 25%, will increase if healthy worker effects are estimated. As these uncertainties are greater than those of the space environmental models and are at about the same level of uncertainty that was estimated for radiation transport codes, they should not be ignored.

Risk in Context of Exploration Mission Operational Scenarios

The accuracy of GCR environmental models, transport codes, and nuclear interaction cross sections, as described above, allow NASA to make predictions of the space environments and organ exposures that will be encountered on missions to the moon or Mars. However, major questions arise due to the lack of knowledge on biological effects. For cancer risk projections, propagating individual uncertainties in factors that enter risk model calculations is used to place reasonable bounds on the cancer risks that will be encountered.

Figure 4-15 shows predictions for the Mars surface. In this figure, the upward neutron flux, which is not included, is judged to carry the largest uncertainty in physics models for exploration. The variation in doses is due to the variation in atmospheric height at different geographic locations (Saganti et al., 2004).

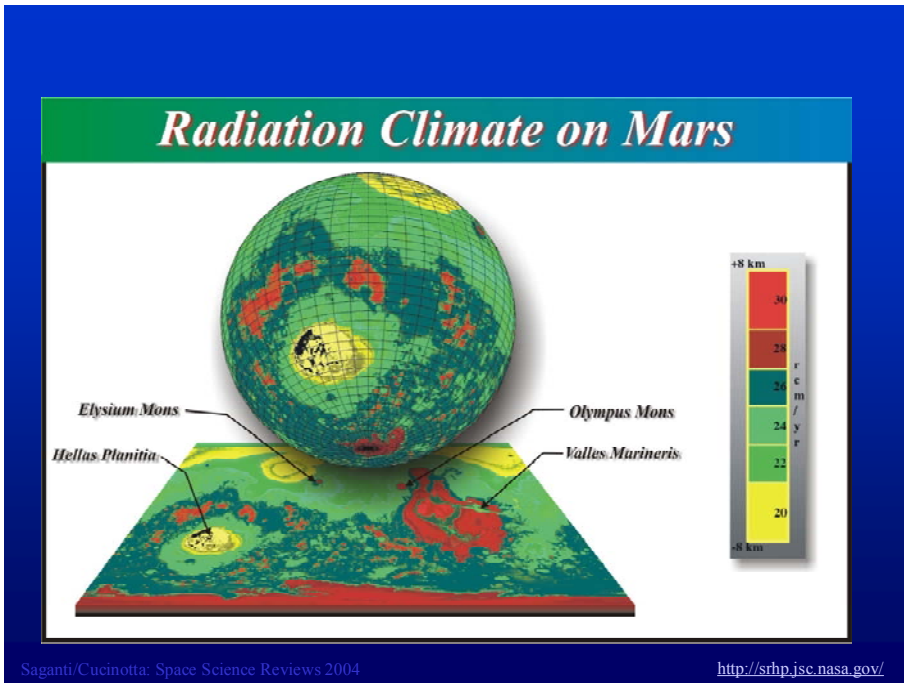

Figure 4-15. ***From Saganti et al. (2004) Predictions of skin dose-equivalent as a function of position on the Mars surface. Atmospheric data are taken from the MOLA [Mars orbiter laser altimeter] experiment.***

PDFs for space exploration missions

The cancer risk projection for space missions is found by folding predictions of the tissue-weighted LET spectra behind spacecraft shielding, dF/dL, with the radiation cancer mortality rate to form a rate for a trial J.

$$m_J(E,a_E,a) = m_{IJ}(E,a_E,a)\int dL\frac{dF}{dL}LQ_{trial-J}(L)x_{L-J} \tag{16}$$

(Not shown are the quantiles that are associated with the low-LET mortality rate.) Alternatively, particle-specific energy spectra, $F_j(E)$, for each ion, j, can be used.

$$m_J(E,a_E,a) = m_{IJ}(E,a_E,a)\sum_j\int dEF_j(E)L(E)Q_{trial-J}(L(E))x_{L-J} \tag{17}$$

The result of Eq(16) or Eq(17) is then inserted into the expression for the REID of Eq(10). In implementing a numerical procedure, we group the PDFs that are related to the risk coefficient of the normal form, which consist of the dosimetry, bias, and statistical uncertainties, into a combined PDF, P_{cmb}(x). After accumulating sufficient trials (~10^5), the results for the REID estimates are binned, and the median values and confidence intervals are found.

We use the χ^2 test for determining whether the PDFs for two distinct shielding configurations or materials are significantly different. We denote the calculated PDFs for a REID of R_i for two configurations or materials as

$p_1(R_i)$ and $p_2(R_i)$, respectively. Each $p(R_i)$ follows a Poisson distribution with variance, $\sqrt{p(R_i)}$. The chi-squared, χ^2 test for n-degrees of freedom characterizing the dispersion between the two distributions is then

$$\chi^2 = \sum_n \frac{[p_1(R_n) - p_2(R_n)]^2}{\sqrt{p_1^2(R_n) + p_2^2(R_n)}} \quad (18)$$

Once χ^2 is determined, the probability P(n, χ^2) that the two distributions are the same is calculated. If χ^2 is sufficiently large such that P(n, χ^2) is less than about 20%, this indicates that we can conclude that the two distributions lead to distinct cancer risks from GCR and/or SPEs, with the material with the lowest mean and upper 95% CL values preferred for radiation protection. However, the opposite result indicates that either the materials are approximately the same, or that the uncertainties in risk models prevent us from concluding that either configuration or material is superior in radiation protection properties. We therefore evaluate χ^2 for the LET-dependent parts of the uncertainties (i.e., quality factors and physics) separately, as only these contributions explicitly depend on the modification of radiation fields by shielding. Tables 4-15 and 4-16 show fatal cancer risk projections at solar minimum for males and females of age 40 years at the time of the mission. Cancer morbidity risks that are about 50% higher than mortality risks are described here. Calculations are made for minimally shielded spacecraft of 5-g/cm^2 aluminum and a heavily shielded spacecraft of 20 g/cm^2. Similar calculations that are near solar maximum are shown in Tables 4-17 and 4-18; an SPE fluence that is equivalent to the August 1972 SPE is assumed to have occurred. At solar minimum, it is seen that a four-fold addition of mass reduces the cancer risk by only about 15%.

Table 4-15. ***Calculations of Effective Doses, REID, and 95% C.I. for Lunar or Mars Missions. Calculations Are at Solar Minimum for a 5-g/cm^2 Aluminum Shield***

Exploration Mission	D, Gy	E, Sv	REID(%)	95% C.I.
	Males (40 years)			
Lunar-long	0.06	0.017	0.68	[0.20, 2.4]
Mars swing-by	0.37	1.03	4.0	[1.0, 10.5]
Mars surface	0.42	1.07	4.2	[1.3, 13.6]
	Females (40 years)			
Lunar-long	0.06	0.17	0.82	[0.23, 3.1]
Mars swing-by	0.37	1.03	4.9	[1.4, 16.2]
Mars surface	0.42	1.07	5.1	[1.6, 16.4]

Table 4-16. ***Calculations of Effective Doses, REID, and 95% C.I. for Lunar or Mars Missions. Calculations Are at Solar Minimum for a 20-g/cm^2 Aluminum Shield***

Exploration Mission	D, Gy	E, Sv	REID(%)	95% C.I.
	Males (40 years)			
Lunar-long	0.06	0.14	0.57	[0.18, 1.9]
Mars swing-by	0.36	0.87	3.2	[1.0, 10.4]
Mars surface	0.41	0.96	3.4	[1.1, 10.8]
	Females (40 years)			
Lunar-long	0.06	0.14	0.68	[0.22, 2.4]
Mars swing-by	0.36	0.87	3.9	[1.2, 12.7]
Mars surface	0.41	0.96	4.1	[1.3, 13.3]

Results differ at solar maximum, where a four-fold increase in shielding mass leads to a more than two-fold reduction in cancer risk and solar protons (Tables 4-17 and 4-18), which are less penetrating than GCR, are effectively mitigated by shielding. However, for heavy shielding ($\geq$ 20 g/cm^2), GCR dominates over SPEs and the further addition of shielding provides marginal reductions. Each SPE is unique in that it has distinct fluence, energy spectra, and dose-rates; the shielding thickness where GCR doses exceed SPE doses therefore varies from event to event. Cancer incidence projections (not shown) are about 60% higher than those listed in these tables. Tables 4-17 and 4-18 show that cancer risk estimates still exceed the PELs for many Exploration mission scenarios and will remain as such until the uncertainties are reduced.

Table 4-17. ***Calculations of Effective Doses, REID, and 95% C.I. for Lunar or Mars Missions. Calculations Are Near Solar Maximum, Assuming 1972 SPE in the Deep Space Segment of the Mission with a 5-g/cm^2 Aluminum Shield***

Exploration Mission	D, Gy	E, Sv	REID(%)	95% C.I.
	Males (40 years)			
Lunar-long	0.49	0.74	3.0	[0.95, 7.9]
Mars swing-by	0.62	1.21	4.4	[1.5, 13.1]
Mars surface	0.66	1.24	4.8	[1.6, 14.2]
	Females (40 years)			
Lunar-long	0.49	0.74	3.6	[1.1, 9.6]
Mars swing-by	0.62	1.21	5.7	[1.8, 17.1]
Mars surface	0.66	1.24	5.8	[2.0, 17.3]

Table 4-18. ***Calculations of Effective Doses, REID, and 95% C.I. for Lunar or Mars Missions. Calculations Are Near Solar Maximum, Assuming 1972 SPE in the Deep Space Segment of the Mission with a 20-g/cm^2 Aluminum Shield***

Exploration Mission	D, Gy	E, Sv	REID(%)	95% C.I.
	Males (40 years)			
Lunar-long	0.08	0.18	0.72	[0.24, 2.4]
Mars swing-by	0.22	0.54	2.0	[0.60, 6.8]
Mars surface	0.25	0.60	2.4	[0.76, 7.8]
	Females (40 years)			
Lunar-long	0.08	0.18	0.86	[0.26, 2.8]
Mars swing-by	0.22	0.54	2.5	[0.76, 8.3]
Mars surface	0.25	0.60	2.9	[0.89, 9.5]

Biological and physical countermeasures

Identifying effective countermeasures with which to reduce the biological damage that is produced by radiation remains a long-term goal of space research. As noted by Durante and Cucinotta (2008), such countermeasures may not be needed for a lunar base, but they probably will be for the Mars mission and definitely will be needed for exploring Jupiter, the Saturn moon Titan, or the nearby satellites. In all of the basic radioprotection textbooks, the authors have stated that there are three means to reduce exposure to ionizing radiation: increasing the *distance* from the radiation source, reducing the exposure *time*, and through use of *shielding*. Distance plays no role in space, as space radiation is omnidirectional. The time that will be spent in space by human crews is likely to be increased rather than decreased, given the plans for exploration and colonization. Shielding remains a plausible countermeasure, albeit a prohibitively costly one in light of current launch mass capabilities. Furthermore, the present uncertainties in risk projection prevent us from determining the true benefit of shielding. Other strategies can be effective in reducing exposure, or the effects of the irradiation, in space. These strategies include the choice of an appropriate time of flight, administration of drugs or dietary supplements to reduce the radiation effects, and crew selection.

Radioprotective Agents

The search for efficient radioprotectors is a major goal of research in radiation protection and therapy. Both radiation injury and oxygen poisoning occur through the formation of reactive oxygen species; therefore, antioxidants can be efficiently used to prevent the damage (Weiss and Landauer, 2003).

As summarized by Durante and Cucinotta (2008),

> "Phosphorothioates and other aminothiols, which are usually administered shortly before irradiation, are so effective in tissue protection against ionizing radiation that one specific compound (Ethyol, also known as amifostine or WR-2721) is approved in many countries for clinical use during chemotherapy and radiotherapy cancer treatments (Sasse et al., 2006). Unfortunately, amifostine (WR-2721) and other thiols have significant side effects, including nausea, vomiting, vasodilatation, and hypotension (Boccia et al., [sic] 2002), precluding their use in spaceflights. Natural occurring antioxidants are less effective than phosphorothioate agents in protection against high-dose acute radiation burden. However, nutritional antioxidants have a low toxicity, can be used for prolonged time, and they seem to play a key role in the prevention of cancer (Halliwell, 2000; Bingham and Riboli, 2004). A diet rich in fruit and vegetables significantly reduced the risk of cancer in the A-bomb survivor

cohort (Sauvaget et al., 2004). Retinoids and vitamins (A, C, and E) are probably the most well-known and studied natural radioprotectors, but hormones (e.g. melatonin), gluthatione, superoxide dismutase, phytochemicals from plant extracts (including green tea and cruciferous vegetables), and metals (especially selenium, zinc, and copper salts) are also under study as dietary supplements for individuals overexposed to radiation (Weiss and Landauer, 2000), including astronauts. In addition, there is evidence of a reduced antioxidant capacity during spaceflight, as shown by reduced superoxide dismutase (SOD) and total antioxidant activity in some astronauts returning from missions on the International Space Station (Smith et al., 2005).

"Understanding the effectiveness of antioxidants in space is complicated by the presence of HZE particles. In principle, antioxidants should provide reduced or no protection against the initial damage from densely ionizing radiation, because the direct effect is more important than free radical-mediated indirect radiation damage at high LET. However, there is an expectation that some benefits should occur for persistent oxidative damage related to inflammation and immune responses. Some recent experiments suggest at least for acute high dose irradiation that an efficient radioprotection by dietary supplements can be achieved even in case of exposure to high-LET radiation. Ascorbate reduces the frequency of mutations in human-hamster hybrid cells exposed to high-LET C-ions (Waldren et al., 2004). Vitamin A strongly reduces the induction of fibroma in rats exposed to swift Fe-ions (Burns et al., 2007). Dietary supplementation with Bowan-Birk protease inhibitors (Guan et al., 2006), L-selenomethionine or a combination of selected antioxidant agents (Kennedy et al., 2007) could partially or completely prevent the decrease in the total antioxidant status in the plasma of mice exposed to proton or HZE particle radiation, and neoplastic transformation of human thyroid cells in vitro. However, because the mechanisms of biological effects are different for low dose-rate compared to acute irradiation, new studies for protracted exposures will be needed to understand the potential benefits of biological countermeasures."

Even if antioxidants can act as radioprotectors, this does not necessarily translate as an advantage for cancer risk. If antioxidants protect cells by rescuing them from apoptosis, this may allow the survival of damaged cells, which eventually can initiate tumor progression. Concern about this possibility is sustained by a recent meta-study of the effects of antioxidant supplements in the diet of normal subjects (Bjelakovic et al., 2007). The authors of this study did not find statistically significant evidence that antioxidant supplements have beneficial effects on mortality. On the contrary, these authors concluded that β-carotene, vitamin A, and vitamin E seem to increase the risk of death. Concerns not only include rescuing cells that still sustain DNA mutations, but also the altered methylation patterns that can result in genomic instability (Kovalchuk et al., 2004). An approach to target damaged cells for apoptosis may be advantageous for chronic exposures to galactic cosmic radiation. Radioprotectors tested for acute exposures at high doses should be used with care – rescuing cells may make the problem worse in the long term.

Shielding

For terrestrial radiation workers, additional protection against radiation exposure is usually provided through increased shielding. Unfortunately, shielding in space is problematic, especially when GCRs are considered. High-energy radiation is very penetrating: a thin or moderate shielding is generally efficient in reducing the equivalent dose, but, as the thickness increases, shield effectiveness drops. This is the result of the production of a large number of secondary particles, including neutrons, that are caused by nuclear interactions of the GCR with the shield. These particles have generally lower energy, but they can have higher quality factors than incident cosmic primary particle. Radiation shielding effectiveness depends on the atomic constituents of the material that is used. Shielding effectiveness per unit mass, which is the highest for hydrogen, decreases with increasing atomic number (Wilson et al. 1995). Liquid hydrogen would display the maximum performance as shield material, but it is not practical since it is a low-temperature liquid. Instead, polyethylene could be a good compromise. Secondary neutron production increases with the mass number of the atomic constituents of the

material and can grow to be large values for materials such as aluminum or the regolith on the martian surface, or for heavier materials such as lead. Unfortunately, most of the biologically dangerous secondary radiation is produced in tissue by very-high-energy GCR nuclei, even behind hydrogen shielding.

For SPE shielding, the situation is much better, and the majority of events on record can be reduced to reasonable dose levels (< 100 mSv) with localized shielding of polyethylene inside a lightly shielded vehicle or habitat (figure 4-16).

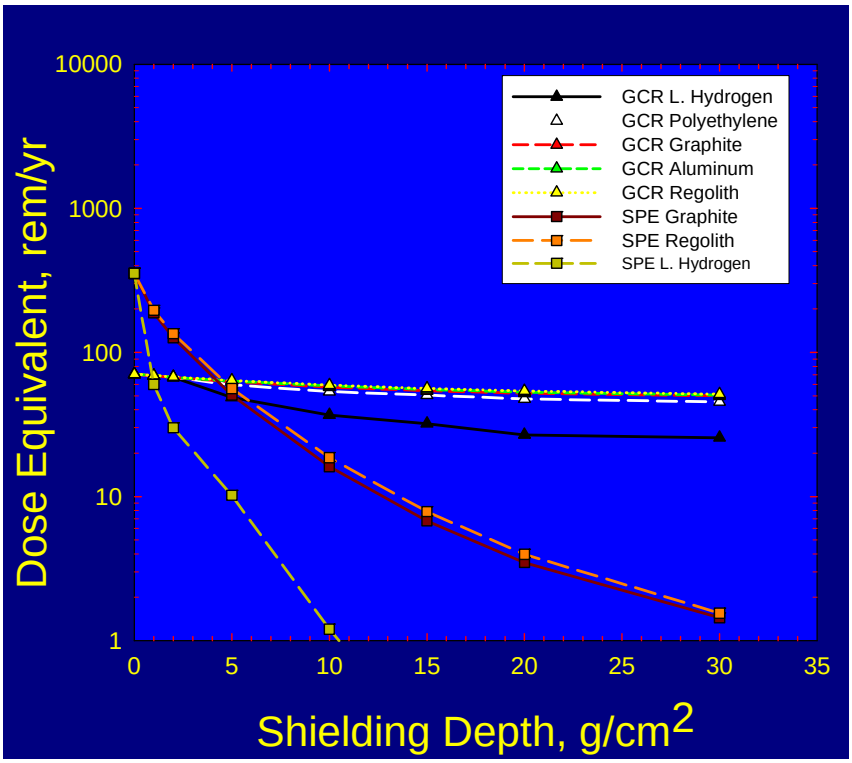

Figure 4-16. ***Effective doses vs. depth in several materials for GCR at solar minimum and the 1972 SPE (Cucinotta et al., 2006).***

Conclusion

The evidence for cancer risks from humans who are exposed to low-LET radiation is extensive for doses above 100 mSv. There are important uncertainties for low-LET radiation at lower doses (<100 mSv), for low dose-rates, and in transferring risks among populations that have different genetic, dietary, etc. attributes. Although human epidemiology can be applied to space exposures, additional uncertainties are related to the quality of radiation in space that is known to produce both qualitative and quantitative differences compared to low-LET radiation in experimental models. The doses that are to be expected on space missions, and the nuclear type and energies, are well understood. NASA has existing models that quite accurately determine radiation physics parameters in space. Reducing the uncertainties in risk assessment, which is required before a mission to Mars can be undertaken, has led to a number of investigations that are guided by molecular and genetic research on carcinogenesis and degenerative diseases. The large uncertainties in risk projection models will only be reduced by improving our basic understanding of the underlying biological processes and their disruption by space radiation. There are unique aspects involved in this approach due to the specific challenges to biological systems that are presented by space radiation, especially HZE ions. It is unlikely that the radiation risk problem for space exploration will be solved by a simple countermeasure, such as shielding or radioprotective drugs. Rather, the risk will be understood and controlled only with more basic research in the field of cancer induction by charged particles (Cucinotta and Durante, 2006).

References

Ainsworth EJ. (1986) Early and late mammalian responses to heavy charged particles. *Adv. Space Res.* 6:153–165.

Alpen EL, Powers-Risius P, Curtis SB, DeGuzman R. (1993) Tumorigenic potential of high-Z, high-LET charged-particle radiations. *Radiat. Res.,* 136:382–391.

Alpen EL, Powers-Risius P, Curtis SB, DeGuzman R, Fry RJM. (1994) Fluence-based relative biological effectiveness for charged particle carcinogenesis in mouse Harderian gland. *Adv. Space Res.,* 14:573–581.

Badhwar GD, O'Neill PM. (1994a) Long-term modulation of galactic cosmic radiation and its model for space exploration. *Adv. Space. Res*., 14(10):749–757.

Badhwar GD, Cucinotta FA, O'Neill PM. (1994b) An analysis of interplanetary space radiation exposure for various solar cycles. *Radiat. Res.,* 138:201–208.

Badhwar GD. (1997) Spaceflight validation of material shielding properties. In: Wilson JW, Miller J, Konradi A, Cucinotta FA (Eds.), *NASA workshop on shielding strategies for human space exploration*. NASA-CP-1997-3360. NASA Johnson Space Center, Houston.

Badhwar GD, Cucinotta FA. (2000) A comparison of depth dependence of dose and linear energy transfer spectra in aluminum and polyethylene. *Radiat. Res.,* 153:1–8.

Barcellos-Hoff MH, Park C, Wright EG. (2005) Radiation and the microenvironment – tumorigenesis and therapy. *Nat. Rev. Canc.,* 5:867–875.

BEIR. Committee to Assess Health Risks from Exposure to Low Levels of Ionizing Radiation. National Research Council of the National Academies. (2006) *Health risks from exposure to low levels of ionizing radiation: BEIR VII – Phase 2*. The National Academies Press, Washington, D.C.

Belli M, Cera F, Cherubini R, Haque AMI, Ianzini F, Moschini G, Sapora O, Simone G, Tabocchini MA, Tiverton P. (1993) Inactivation and mutation induction in V79 cells by low energy protons: re-evaluation of the results at the LNL facility. *Int. J. Radiat. Biol*., 63:331–337.

Billings MP, Yucker WR, Heckman BR. (1973) *Body self-shielding data analysis*. MDC-G4131. McDonnell-Douglas Astronautics Company West.

Bingham S, Riboli E. (2004) Diet and cancer—the European prospective investigation into cancer and nutrition. *Nat. Rev. Canc.,* 4:206–215.

Bjelakovic G, et al. (2007) Mortality in randomized trials of antioxidant supplements for primary and secondary prevention: systematic review and meta-analysis. *J. Am. Med. Assoc*., 297:842–857.

Boccia R. (2002) Improved tolerability of amifostine with rapid infusion and optimal patient preparation. *Semin. Oncol.,* 29:S9–S13.

Bunger BM, Cook JR, Barrick MK. (1981) Life table methodology for evaluating radiation risk: an application based on occupational exposures. *Health Phys.,* 40:439–455.

Burns FJ, Jin Y, Koenig KL, Hosselet S. (1993) The low carcinogenicity of electron radiation relative to argon ions in rat skin. *Radiat. Res.,* 135:178–188.

Burns F, Yin Y, Garte SJ, Hosselet S. (1994) Estimation of risk based on multiple events in radiation carcinogenesis of rat skin. *Adv. Space Res.,* 14:507–519.

Burns FJ, et al. (2007) Induction and prevention of carcinogenesis in rat skin exposed to space radiation. *Radiat. Environ. Biophys.,* 46:195–199.

Campisi J. (2003) Cancer and aging: rival demons. *Nat. Rev. Canc.,* 3:339–349.

Campisi J, d'Adda di Fagagna F. (2007) Cellular senescence: when bad things happen to good cells. *Nat. Rev. Mol. Cell. Biol.,* 8:729–740.

Cardis E, et al. (1995) Effects of low doses and dose-rates of external ionizing radiation: cancer mortality among nuclear industry workers in three countries. *Radiat. Res.,* 142:117–132.

Cardis E, et al. (2007) The 15-country collaborative study of cancer risks among radiation workers in the nuclear industry: estimates of radiation-related cancer risks. *Radiat. Res.,* 167:396–416.

Chang PY, Bjornstad KA, Rosen CJ, et al. (2005) Effects of iron ions, protons and X rays on human lens cell differentiation. *Radiat. Res.,* 164:531–539.

Cox R, Masson WK. (1979) Mutation and inactivation of cultured mammalian cells exposed to beams of accelerated heavy ions. *Int. J. Radiat. Biol.,* 36:149–160.

Cucinotta FA, Wilson JW, Shavers MR, Katz R. (1996) Effects of track structure and cell inactivation on the calculation of heavy ion mutation rates in mammalian cells. *Int. J. Radiat. Biol.,* 69:593–600.

Cucinotta FA, Wilson JW, Shinn JL, Tripathi RK. (1998a) Assessment and requirements of nuclear reaction data bases for gcr transport in the atmosphere and structures. *Adv. Space Res.,* 21:1753–1762.

Cucinotta FA, Nikjoo H, Goodhead DT. (1998b) Comment on the effects of delta-rays on the number of particle-track transversals per cell in laboratory and space exposures. *Radiat. Res.,* 150:115–119.

Cucinotta FA, Nikjoo H, Goodhead DT. (2000a) Model of the radial distribution of energy imparted in nanometer volumes from HZE particles. *Radiat. Res*., 153:459–468.

Cucinotta FA, Wilson JW, Williams JR, Dicello JF. (2000b) Analysis of *Mir*-18 results for physical and biological dosimetry: radiation shielding effectiveness in LEO. *Radiat. Meas.,* 31:181–191.

Cucinotta FA, Schimmerling W, Wilson JW, Peterson LE, Saganti P, Badhwar GD, Dicello JF. (2001) Space radiation cancer risks and uncertainties for Mars missions. *Radiat. Res.,* 156:682–688.

Cucinotta FA, Badhwar GD, Saganti P, Schimmerling W, Wilson JW, Peterson L, Dicello J. (2002) *Space radiation cancer risk projections for exploration missions, uncertainty reduction and mitigation*. NASA TP-2002-210777. NASA Johnson Space Center, Houston.

Cucinotta FA, Wu H, Shavers MR, George K. (2003a) Radiation dosimetry and biophysical models of space radiation effects. *Grav. Space Biol. Bull*., 16:11–18.

Cucinotta FA, Saganti PB, Hu X, Kim M-HY, Cleghorn TF, Wilson JW, Tripathi RK, Zeitlin CJ. (2003b) *Physics of the isotopic dependence of galactic cosmic ray fluence behind shielding*. NASA TP-2003-210792. NASA Johnson Space Center, Houston.

Cucinotta FA, Kim MH, Ren L. (2006) Evaluating shielding effectiveness for reducing space radiation cancer risks. *Radiat, Meas.,* 41:1173–1185.

Cucinotta FA, Durante M. (2006) Cancer risk from exposure to galactic cosmic rays: implications for space exploration by human beings. *Lancet Oncol*., 7:431–435.

Cucinotta FA, Kim MY, Willingham V, George KA. (2008) Physical and biological dosimetry analysis from International Space Station astronauts. *Radiat. Res.*, 170:127–138.

Dicello J.F, et al. (2004) In vivo mammary tumorigenesis in the Sprague-Dawley rat and microdosimetric correlates. (2004) *Phys. Med. Biol.,* 49:3817–3830.

Ding L, Shingyoji M, Chen F, et al. (2005) Gene expression changes in normal human skin fibroblasts induced by HZE-particle radiation. *Radiat. Res.,* 164:523–526.

Durante M, George K, Wu H, Cucinotta FA. (2002) Karyotypes of human lymphocytes exposed to high-energy iron ions. *Radiat. Res.,* 158:581–590.

Durante M, Kronenberg A. (2005) Ground-based research with heavy ions for space radiation protection. *Adv. Space Res.,* 35:180–184.

Durante M, Cucinotta FA. (2008) Heavy ion carcinogenesis and human space exploration. *Nat. Rev. Canc.,* 8(6):465–472.

Feldser DM, Hackett JA, Greider CW. (2003) Telomere dysfunction and the initiation of genome instability. *Nat. Rev. Canc.,* 3:623–627.

Flint-Richter P, Sadetzki S. (2007) Genetic predisposition for the development of radiation-associated meningioma: an epidemiological study. *Lancet Oncol.,* 8:403–410.

Folkman J, Watson K, Ingber D, Hanahan D. (1989) Induction of angiogenesis during the transition from hyperplasia to neoplasia. *Nature,* 339:58–61.

Fry RJM, Powers-Risius P, Alpen EL, Ainsworth EJ. (1985) High LET radiation carcinogenesis. *Radiat. Res.,* 104:S188–S195.

Fry RJM, Storer JB. (1987) External radiation carcinogenesis. *Adv. Radiat. Biol.,* 13:31–91.

George K, et al. (2001) Chromosome aberrations in the blood lymphocytes of astronauts after spaceflight. *Radiat. Res.,* 156:731–738.

George K, Durante M, Willingham V, Wu H, Yang T, Cucinotta FA. (2003) Biological effectiveness of accelerated particles for the induction of chromosome damage measured in metaphase and interphase human lymphocytes. *Radiat. Res.,* 160:425–435.

George KA, Hada M, Jackson LJ, Elliott T, Kawata T, Pluth JM, Cucinotta FA. (2009) Dose response of gamma rays and iron nuclei for induction of chromosomal aberrations in normal and repair-deficient cell lines. *Radiat. Res.,* 171(6):752–763.

Goodhead DT. (1994) Initial events in the cellular effects of ionizing radiations: clustered damage in DNA. *Int. J. Radiat. Biol.,* 65:7–17.

Guan J, et al. (2006) Effects of dietary supplements on the space radiation-induced reduction in total antioxidant status in CBA mice. *Radiat. Res.,* 165:373–378.

Hall EJ, et al. (2006) The relative biological effectiveness of densely ionizing heavy-ion radiation for inducing ocular cataracts in wild type versus mice heterozygous for the ATM gene. *Radiat. Environ. Biophys.,* 45:99–104.

Hall EJ. (2007) Cancer caused by x-rays—a random event? *Lancet Oncol.,* 8:369–370.

Halliwell B. (2000) The antioxidant paradox. *Lancet,* 375:1179–1180.

Hanahan D, Weinberg, RA. (2000) The hallmarks of cancer. *Cell,* 100:57–70.

Huang L, Snyder AR, Morgan WF. (2003) Radiation-induced genomic instability and its implications for radiation carcinogenesis. *Oncogene,* 22:5848–5854.

International Atomic Energy Agency. (2001) Cytogenetic analysis for radiation dose assessment. IAEA Technical Report No. 405. IAEA, Vienna, Austria.

ICRP. (1991) *Recommendations of the International Commission on Radiation Protection*. ICRP Publication No. 60. Annals of the ICRP 21. Elsevier Science, N.Y.

ICRP. (2003) *Relative biological effectiveness (RBE), quality factor (Q), and radiation weighting factor (w_R)*. ICRP Publication No. 92. Pergamon Press, Oxford, U.K.

ICRU. (1986) *The quality factor in radiation protection*. ICRU Report No. 40. ICRU Publications, Bethesda, Md.

Katz R, Ackerson B, Homayoonfar M, Scharma SC. (1971) Inactivation of cells by heavy ion bombardment. *Radiat. Res.,* 47:402–425.

Kawata T, Durante M, Furusawa Y, George K, Takai N, Wu H, Cucinotta FA. (2001) Dose response of initial G2-chromosomal damage induced in normal human fibroblasts by high-LET particles. *Int. J. Radiat. Biol.,* 77:165–174.

Kennedy AR, Guan J, Ware JH. (2007) Countermeasures against space radiation induced oxidative stress in mice. *Radiat. Environ. Biophys*., 46:201–203.

Kiefer J, Stoll U, Schneider E. (1994) Mutation induction by heavy ions. *Adv. Space Res*., 14(10):257–265.

Kiefer J, Pross HD. (1999) Space radiation effects and microgravity. *Mutat. Res.,* 430:299–305.

Kiefer J. (2002) Mutagenic effects of heavy charged particles. *J. Radiat. Res.,* 43:S21–S25.

Kim MY, Barber RE, Shavers MR, Nikjoo H, Cucinotta FA. (2003) *TEPCs overestimate the average quality factor for trapped protons and underestimate the average quality factor for GCR*. Presented at the 14th Annual Space Radiation Health Investigators Workshop. April 27–30. South Shore Harbour Resort and Conferece Center, League City, Texas.

Kovalchuk O, et al. (2004) Methylation changes in muscle and liver tissues of male and female mice exposed to acute and chronic low-dose X-ray-irradiation. *Mutat. Res.,* 548:75–84.

Kronenberg A. (1994) Mutation induction in human lymphoid cells by energetic heavy ions. *Adv. Space Res.,* 14(10):339–346.

Kronenberg A, Gauny S, Criddle K, et al. (1995) Heavy ion mutagenesis: linear energy transfer effects and genetic linkage. *Radiat. Environ. Biophys.,* 34:73–78.

Martin SG, Miller RC, Geard CR, Hall EJ. (1995) The biological effectiveness of radon-progeny alpha particles. IV. Morphological transformation of syrian hamster embryo cells at low dose. *Radiat. Res.,* 142:70–77.

Mase RS, DePinho RA. (2002) Connecting chromosomes, crisis, and cancer. *Science,* 297:565–569.

Miller RC, Marino SA, Brenner DJ, Martin SG, Richards M, Randers-Pehrson G, Hall EJ. (1995) The biological effectiveness of radon-progeny alpha particles. III. Quality factors. *Radiat. Res.,* 142:61–69.

Mothersill C, Seymour CB. (2004) Radiation-induced bystander effects- implications for cancer. *Nat. Rev. Canc.,* 4:158–164.

National Academy of Sciences Committee on Biological Effects of Ionizing Radiation. (2005) *Health risks from exposure to low levels of ionizing radiation. BEIR VII*. National Academy Press, Washington, D.C.

NCRP. (1989) *Guidance on radiation received in space activities*. NCRP Report No. 98. NCRP, Bethesda, Md.

NCRP. (1990) *Relative biological effectiveness of radiations of different quality*. NCRP Report No. 104. NCRP, Bethesda, Md.

NCRP. (1997a) *Uncertainties in fatal cancer risk estimates used in radiation protection*. NCRP Report No. 126. NCRP, Bethesda, Md.

NCRP. (1997b) Acceptability of risk from radiation – application to human spaceflight. NCRP Symposium Proceedings No. 3, held on May 29, 1996, Arlington, Va. NCRP, Bethesda, Md.

NCRP. (2000) *Recommendations of dose limits for low Earth orbit*. NCRP Report No. 132. NCRP, Bethesda, Md.

NCRP. (2005) *Extrapolation of radiation-induced cancer risks from nonhuman experimental systems to humans*. NCRP Report No. 150. Bethesda, Md.

NCRP. (2006) *Information needed to make radiation protection recommendations for space missions beyond low-Earth orbit*. NCRP Report No. 153. NCRP, Bethesda, Md.

Nelson GA, Schubert WW, Marshall TM, Benton ER, Benton EV. (1989) Radiation effects in *caenorhabditis elegans*, mutagenesis by high and low LET ionizing radiation. *Mutat. Res.,* 212:181–192.

Nikjoo H, O'Neill P, Terrissol M, Goodhead DT. (1999) Quantitative modeling of DNA damage using Monte Carlo track structure method. *Radiat. Envir. Biophys.,* 38:31–38.

Nikjoo H, Khvostunov IK, Cucinotta FA. (2002) The response of (TEPC) proportional counters to heavy ions. *Radiat. Res.,* 157:435–445.

NRC. (1967) *Radiobiological factors in manned spaceflight, report of Space Radiation Study Panel of the Life Sciences Committee*. Langham WH (Ed.). National Academy Press, Washington, D.C.

NRC. (1970) *Radiation protection guides and constraints for space-mission and vehicle-design studies involving nuclear system, Report of the Radiobiologic Advisory Panel of the Committee on Space Medicine Space Science Board*. Langham WH, Grahn D (Eds.). National Academy Press, Washington, D.C.

O'Neill P. (2005) Badhwar-O'Neill galactic cosmic ray model update based on advanced composition explorer (ACE) spectra from 1997 to present. *Adv. Space Res.,* 37(9):1727–1733.

Park CC, et al. (2003) Ionizing radiation induces heritable disruption of epithelial cell interactions. *Proc. Natl. Acad. Sci. Unit. States Am.,* 100:10728–10733.

Parker EN. (1965) The passage of energetic charged particles through interplanetary space. *Planet. Space Sci.,* 13:9–49.

Pierce DA, Shimizu Y, Preston DL, Vaeth M, Mabuchi K. (1996) Studies of the mortality of the atomic-bomb survivors. Report 12, Part I. Cancer: 1950–1990. *Radiat. Res.,* 146:1–27.

Pluth JM, et al. (2008) DNA double strand break repair and chromosomal rejoining defects with misrejoining in Nijmegen breakage syndrome cells. *DNA Repair.,* 7:108–118.

Ponder BA. (2001) Cancer genetics. *Nature,* 411:336–341.

Preston DL, Mattsson A, Holmberg A, Shore R, Hilddreth NG, Boice JD. (2002) Radiation effects on breast cancer risk: a pooled analysis of eight cohorts. *Radiat. Res.,* 158:220–235.

Preston DL, Shimizu Y, Pierce DA, et al. (2003) Studies of mortality of atomic bomb survivors. Report 13: Solid cancer and non-cancer disease mortality: 1950–1997. *Radiat. Res.,* 160:381–407.

Preston DL, et al. (2007) Solid cancer incidence in atomic bomb survivors: 1958–1998. *Radiat. Res.,* 168:1–64.

Prise KM, et al. (1998) A review of Dsb induction data for varying quality radiations. *Int. J. Radiat. Biol.,* 74:173–184.

Riballo E, et al. (2004) A pathway of double-strand break rejoining dependent upon ATM, Artemis and proteins locating to γ-H2AX foci. *Mol. Cell,* 16:715–724.

Rydberg B, Cooper B, Cooper PK, et al. (2005) Dose-dependent misrejoining of radiation-induced DNA double-strand breaks in human fibroblasts: experimental and theoretical study for high- and low-LET radiation. *Radiat. Res.,* 163:526–534.

Sabatier L, Dutrillaux B, Martin M. (1992) Chromosomal instability. *Nature,* 357:548.

Sabatier L, Ricoul M, Pottier G, Murnane JP. (2005) The loss of a single telomere can result in instability of multiple chromosomes in a human tumor cell line. *Mol. Canc. Res.,* 3:139–150.

Saganti PB, Cucinotta FA, Wilson JW, et al. (2004) Radiation climate map for analyzing risks to astronauts on the Mars surface from galactic cosmic rays. *Space Sci. Rev.,* 110:143–156.

Sasse AD, Clark LG, Sasse EC, Clark OA. (2006) Amifostine reduces side effects and improves complete response rate during radiotherapy: results of a meta-analysis. *Int. J. Radiat. Oncol. Biol. Phys.,* 64:784–791.

Sauvaget C, Kasagi F, Waldren CA. (2004) Dietary factors and cancer mortality among atomic-bomb survivors. *Mutat. Res.,* 551:145–152.

Schimmerling W, Cucinotta FA, Wilson JW. (2003) Radiation risk and human space exploration. *Adv. Space Res.,* 31:27–34.

Smilenov LB, Brenner DJ, Hall EJ. (2001) Modest increased sensitivity to radiation oncogenesis in ATM heterozygous versus wild-type mammalian cells. *Cancer Res.,* 61:5710–5713.

Smith SM, et al. (2005) The nutritional status of astronauts is altered after long-term spaceflight aboard the International Space Station. *J. Nutr.,* 135:437–443.

Smyth MJ, Dunn GP, Schreiber RD. (2006) Cancer immunosurveillance and immunoediting: the roles of immunity in suppressing tumor development and shaping tumor immunogenicity. *Adv. Immunol.,* 90:1–50.

SSA. (2004) *A stochastic model of the long-range financial status of the OASDI Program Actuarial Study No. 117*. SSA Pub. No. 11-11555. Office of the Chief Actuary, Washington, D.C.

Sutherland BM, Bennett PV, Sidorkina O, Laval J. (2000) Clustered DNA damages induced in isolated DNA and in human cells by low doses of ionizing radiation. *Proc. Natl. Acad. Sci. Unit. States Am.,* 97:103–108.

Thompson D, et al. (2005) Cancer risks and mortality in heterozygous ATM mutations carriers. *J. Natl. Canc. Inst.,* 97:813–822.

Tsuboi K, Yang TC, Chen DJ (1992) Charged-particle mutagenesis. I: Cytotoxic and mutagenic effects of high-LET charged iron particles on human skin fibroblasts. *Radiat. Res.,* 129:171–176.

Ullrich RL. (1984) Tumor Induction in BAL/c Mice after Fractionated Neutron or Gamma Irradiation. *Radiat. Res*., 93:506–512.

Ullrich RL, Ponnaiya B. (1998) Radiation-induced instability and its relation to radiation carcinogenesis. *Int. J. Radiat. Biol.,* 74:747–754.

Vaeth M, Pierce DA. (1990) Calculating excess lifetime risk in relative risk models. (1990) *Environ. Health Perspect.,* 87:83–94.

Waldren CA, Vannais DB, Ueno AM. (2004) A role for long-lived radicals (LLR) in radiation-induced mutation and persistent chromosomal instability: counteraction by ascorbate and RibCys but not DMSO. *Mutat. Res.,* 551:255–265.

Wang J, et al. (2005) Artemis phosphorylation and function in response to damage. *DNA Repair,* 4:556–570.

Weil M. (2009) Incidence of acute myeloid leukemia and hepatocellular carcinoma in mice irradiated with 1 GeV/nucleon ^{56}Fe Ions. *Radiat Res*., 172: 213–219.

Weiss JF, Landauer MN. (2000) Radioprotection by antioxidants. *Ann. New York Acad. Sci.,* 899:44–60.

Weiss JF, Landauer MR. (2003) Protection against ionizing radiation by antioxidant nutrients and phytochemicals. *Toxicology,* 189:1–20.

Wilson JW, Kim, M, Schimmerling W, Badavi FF, Thibeault SA, Cucinotta FA, Shinn JL, Kiefer R. (1995) Issues in space radiation protection. *Health Phys*., 68:50–58.

Worgul BV, et al. (2002) Atm heterozygous mice are more sensitive to radiation-induced cataracts than are their wild-type counterparts. *Proc. Natl. Acad. Sci. Unit. States Am*., 99:9836–9839.

Yang TCH, Craise LM, Mei MT, Tobias CA. (1985) Neoplastic cell transformation by heavy charged particles. *Radiat. Res.,* 8:S177–S187.

Yang TC, Craise LM, Mei MT, Tobias CA. (1989) Neoplastic cell transformation by high-LET radiation: molecular mechanisms. *Adv. Space Res.*, 9(10):131–140.

Yasuda H, Badhwar GD, Komiyama T, Fujitaka K. (2000) Effective dose equivalent on the ninth shuttle-*Mir* mission (STS 91). *Radiat. Res.,* 154:705–713.

Zhang Q, Williams ES, Askin K, et al. (2005) Suppression of DNA-PK by RNAi has different quantitative effects on telomere dysfunction and mutagenesis in human lymphoblasts treated with gamma-rays or HZE particles. *Radiat. Res.,* 164:497–504.